DANMARKS OG GRØNLANDS GEOLOGISKE UNDERSØGELSE **RAPPORT 2022/29**

CCS2022-2024 WP1: The Inez structure

Seismic data and interpretation to mature potential geological storage of CO_2

Michael B.W. Fyhn, Ulrik Gregersen, Lars Hjelm, Trine D. Jensen, Shahjahan Laghari, Bodil W. Lauridsen, Anders Mathiesen, Finn Mørk, Henrik. I. Petersen, Lasse M. Rasmussen & Niels H. Schovsbo

GEOLOGICAL SURVEY OF DENMARK AND GREENLAND
DANISH MINISTRY OF CLIMATE, ENERGY AND UTILITIES

G E U S

Preface

A new Danish Climate Act was decided by the Danish Government and a large majority of the Danish Parliament on June 26th, 2020. It includes the aim of reducing the Danish greenhouse gas emissions with 70 % by 2030 compared to the level of emissions in 1990. The first part of a new Danish CCS-Strategy of June 30th, 2021 includes a decision to continue the initial investigations of sites for potential geological storage of CO_2 in Denmark. GEUS has therefore from 2022 commenced seismic acquisition and investigations of potential sites for geological storage of CO_2 in Denmark.

The structures decided for maturation by the authorities, are some of the largest structures onshore Zealand, Jutland and Lolland and in the eastern North Sea (Fig. 1.1). The onshore structures include the Havnsø, Gassum, Thorning, and Rødby structures, and in addition the small Stenlille structure as a demonstration/pilot site. The offshore structures include the Inez, Lisa and Jammerbugt structures. A GEUS Report is produced for each of the structures to mature the structure as part of the CCS2022–2024 project towards potential geological storage of CO_2.

The intension with the project reporting for each structure is to provide a knowledge-based maturation with improved database and solid basic descriptions to improve the understanding of the formation, composition, and geometry of the structure. It includes a description overview and mapping of the reservoir and seal formations, the largest faults, the lowermost closure (spill-point) and structural top point of the reservoir, estimations of the overall closure area and gross-rock volume. In addition, the database will be updated, where needed with rescanning of some of the old seismic data, and acquisition of new seismic data in a grid over the structures, except for the Inez and Lisa structures. The study areas of the Lisa and Inez structures are covered by 1784 km and 1577 km of legacy 2D seismic data, respectively, sufficient for their initial investigation. TGS and Danpec A/S graciously made 852 km and 947 km reprocessed proprietary seismic data covering the Lisa and Inez study areas, respectively, available for this study.

The reports will provide an updated overview of the database, geology, and seismic interpretation for all with interests in the structures and will become public available. Each reporting is a first step toward geological maturation and site characterization of the structures. A full technical evaluation of the structures to cover all aspects related to CO_2 storage including risk assessment is recommended for the further process.

Content

Dansk sammendrag

Datagrundlag

Området omkring Inez strukturen er dækket af et net af 2D reflektionsseismiske data af varierende tæthed og datakvalitet med en samlet længde på omkring 1577 km. Hovedparten af data indsamledes i forbindelse med olie-gas efterforskning i 1980'erne. Nihundrede syv og halvfjers linjekilometer som indsamledes i første halvdel af 1980'erne blev siden reprocesseret i 1990'erne og markedsføres af TGS og Danpec A/S, som gjorde dem tilgængelige for studiet. Disse linjer giver en god regional dækning af undersøgelsesområdet og Inez strukturen specifikt. Desuden er strukturen, inklusiv to reservoir- og sejlenheder, gennemboret i Inez-1 brønden. Andre brønde er boret i området og har bidraget til forståelsen af de geologiske lag i og omkring Inez; herunder har særligt Felicia-1 brønden bidraget med information om den dybere geologi, som ikke er boret i Inez-1. De fleste seismiske data anvendt i dette studie er industridata indsamlet i løbet af 1980'erne, og nogle af de regionale seismiske linjer er reprocesseret i 90'erne. Samlet set er den seismiske dækning og kvalitet moderat, men sammen med boringerne dog god nok til at give en overordnet forståelse af Inez strukturens størrelse, grundlæggende geologiske forhold og kritiske elementer, der bør undersøges yderligere.

Tolkning

Inez strukturen er en geologisk 4-vejs lukning dannet som en såkaldt 'skildpadde'-struktur som følge af saltbevægelser og deraf følgende differentieret indsynkning hen over strukturen i særlig Trias og Jura tid. Lukningen findes på forskellige stratigrafiske niveauer, herunder både langs toppen af Haldager Sand, Gassum og Skagerrak formationerne (Fm), som alle tre besidder reservoir egenskaber. De to førstnævnte er boret i Inez-1 og i andre boringer i regionen og indeholder høj-porøse sandstenslag med god permeabilitet og udmærkede net/gross-forhold. Toppen af Haldager Sand og Gassum Fm i Inez-1 ligger i henholdsvis 1524m og 1633m dybde. Reservoirsandet på Haldager Sand Fm-niveau er kun få meter tykt og lukningen har et meget begrænset areal, så lagringspotentialet er på dette niveau begrænset. Potentialet er dog væsentligt større på Gassum Fm-niveau. Den reservoirholdige Gassum Fm måler knap 150 m i tykkelse i Inez-1, heraf tolkes godt halvdelen at bestå af reservoir sand på baggrund af petrofysiske data.

Dybere nede i stratigrafien tolkes tilstedeværelsen af Skagerrak Fm på baggrund af seismisk stratigrafisk tolkning. Enheden er ikke boret i Inez-1, men indeholder et reservoirpotentiale i eksempelvis Felicia-1 brønden, som gennemborer denne typisk meget tykke formation. Porøsitet og permeabilitet forventes dog at være mindre end i den overliggende Gassum Fm pga. den dybere begravelse og pga. et formodentlig mere kompositionelt umodent sediment.

Gassum Fm overlejres af en mere end 100 meter tyk enhed (Fjerritslev Fm) bestående overvejende af tætte mudder- og lersten, som forventes at have gode seglegenskaber. Imidlertid forsætter mindre forkastninger både Gassum Fm (reservoiret) og i hvert fald den nedre del af Fjerritslev Fm-seglet. Der er ikke tegn på igangværende naturlig seismisk aktivitet (jordskælv) i Inez-området, og forkastningssystemet er formentligt inaktivt. Det kan dog have negativ indvirkning på både seglets effektivitet samt Gassum reservoirets sammenhængskraft og dermed samlede lagringseffektivitet. Forkastningerne er hovedsageligt koncentreret over en del af Inez-lukningen.

Inez strukturen forventes på toppen af Skagerrak Fm-niveau at være forsejlet under en tykt udviklet Oddesund Fm. Oddesund Fm indeholder tætte mudderstenlag og evaporitlag, men er ikke boret i Inez-1 brønden. Den er dog tolket til at ligge mellem bunden af brønden og toppen af

Skagerrak Fm på baggrund af seismisk stratigrafisk analyse. Haldager Sand Formationen forventes forseglet af øvre Jura muddersten fra Børglum Formationen.

Inez strukturen har et areal samt en reservoirtykkelse og kvalitet, der gør, at store mængder CO_2 formentlig vil kunne lagres, med det forbehold, at fremtidige undersøgelser kan verificere, at seglene har tilstrækkelig tykkelse, kvalitet og tæthed, også i forhold til forkastninger, til at holde CO_2 fanget i reservoiret, og at Gassum Fm-reservoiret samlet set er sammenhængende nok til, at CO_2 kan injiceres effektivt.

Lagring i Inez kan således formentlig finde sted i alle tre geologiske formationer (Gassum Fm, Haldager Sand Fm og Skagerrak Fm) beliggende i forskellig dybde og adskilt af mellemliggende segl bjergarter. Heraf vurderes det, at de største mængder kan lagres i Gassum Fm, mens lager potentialet i Haldager Sand Fm formentlig er beskedent. Skagerrak Fm kan muligvis bidrage som lager og dermed øge det samlede lager potentiale i Inez. Monte Carlo simulering baseret på en 5% til 15% lagringseffektivitetskoefficient sandsynliggør, at Inez strukturen samlet set formentlig vil kunne indeholde mellem 138 (P90) og 300 (P10) megaton CO_2 (gennemsnit estimat: ca. 214 megaton). Dette estimat afhænger af faktorer, som formentlig vil ændres når nye data indsamles over strukturen og i takt med at den regionale stratigrafiske tolkning forbedres. Estimatet er særligt påvirkeligt af den forventede lagringseffektivitetskoefficient og af det kortlagte lagringsvolumen. Gassum Fm vil jf. dette estimat bidrage med mellem ca. 104 (P90) og 264 (P10) megaton, og anses således at udgøre langt det væsentligste reservoir i Inez strukturen.

Yderligere dataindsamling af bl.a. 3D seismik, kortlægning og detailstudier af reservoirer, segl, forkastninger og andre geologiske risici, vurdering af trykforhold, geomekanik og bjergartsstress, påvirkninger af geokemi og mineraler, modelleringer, detailevalueringer af CO_2 lagringskapacitet, tekniske risici bl.a. ifbm. eksisterende og nye boringer, osv., ligger udover dette projekt, men anbefales udført, f.eks. som led i en yderligere modning og evaluering forud for egentlig lagring.

1. Summary

Permanent CO_2 storage in geological subsurface structures is an efficient way for lowering emissions of greenhouse gases to the atmosphere. The Inez structure is located around 50 km offshore in the northern Danish North Sea and is one of the larger geological structures with a promising storage potential (Fig.1.1). The Inez area is covered by an open 2-D seismic grid of variable quality and the structure was drilled in 1978 by the Inez-1 well as hydrocarbon exploration efforts (Fig.1.2). The Inez structure is a turtle back structure formed in response to Zechstein salt migration and the build-up of six large salt pillow and diapirs during mainly Middle Triassic through Early Cretaceous time next to the Inez structure. The associated differential subsidence caused laterally migrating rim-synclines around the Inez structure, which created a four-way closure at three reservoir levels: (1) Top Skagerrak Formation (Fm); (2); Top Gassum Fm and (3) Top Haldager Sand Fm (Fig.1.3; 1.4). The Gassum and Haldager Sand fms are intersected in the Inez-1 well and include sandstones with average porosities of 20.3% and 26.0%, respectively and derived average permeabilities of 442 mD and 871 mD, respectively. The Rhaetian to Hettangian Gassum Fm deposited in a near-shore environment is here reinterpreted and measures 148 m in thickness in Inez-1. It has a net-to-gross ratio of around 0.59 and is characterized by a c. 300 km^2 mapped closure, while the Middle Jurassic Haldager Sand Fm only measures 9 m in thickness, has a net-to-gross ratio around 0.32 and is characterized by a c. 60 km^2 mapped closure and is therefore considered a secondary reservoir to the Gassum Fm. The two reservoir intervals are overlain by thick claystone intervals. The Lower Jurassic Fjerritslev Fm comprises a 127 m thick claystone-dominated interval in Inez-1 and forms the primary seal for the Gassum Fm. Similarly, the Jurassic sandstone interval is capped by thickly developed Upper Jurassic claystones of the Børglum Formation that form a sealing unit. The Upper Triassic section encountered in Inez-1 is reinterpreted in this study to be composed by a thickly developed Gassum Fm overlying a proximal facies of the Vinding Fm in which the well floors. The Lower to lowermost Upper Triassic Skagerrak Fm interpreted seismically to be present within the Inez structure comprises another secondary reservoir. The top of the Skagerrak Fm has a mapped closure of roughly 150 km^2 and 175m height with a top point presumably located around 2500 m subsurface. The unit is not intersected in the Inez-1, that terminated in the uppermost Triassic, but good reservoir properties is anticipated by analogy to data from Danish wells encountering the Skagerrak Fm elsewhere. The Skagerrak Fm is interpreted to be overlain by mainly fine-grained sediments of the Oddesund Fm that likely comprise a tight sealing unit.

Monte Carlo simulations of the reservoir storage capacity suggest a substantial CO_2 storage potential within the Inez structure. A large mean storage capacity of 178 million ton (MT) CO_2 is modelled for the Gassum Fm, while the Skagerrak Fm is modelled to hold a mean storage capacity of 43 MT CO_2 and the Haldager Sand Fm to hold a mean storage capacity of only 3 MT. In total, an unrisked mean storage potential of the Inez structure of 225 MT CO_2 is modelled for all three reservoir units with a range between 149 MT CO_2 (P90) and 310 MT CO_2 (P10) and a P50 of 216 MT CO_2. A geological risk defined at this stage is associated with densely spaced faulting of the Gassum Fm reservoir offsetting it with typically few tens of meters, which introduces a risk for reservoir compartmentalisation. Faults continue upwards into and the overlying Fjerritslev Fm seal, and although the Fjerritslev Fm seal thickness fully comply with the recommendations for CO_2 storage, the potential risk for leakage along fault planes needs further investigation. Further data acquisition (in particular 3D seismic data) and detailed geological and other technical work (e.g. on pressure/capillary-pressure, geochemistry, stress, geomechanics, seal-integrity, leakage risks at faults and existing/new wells, etc.) are recommended to mature and de-risk the Inez structure.

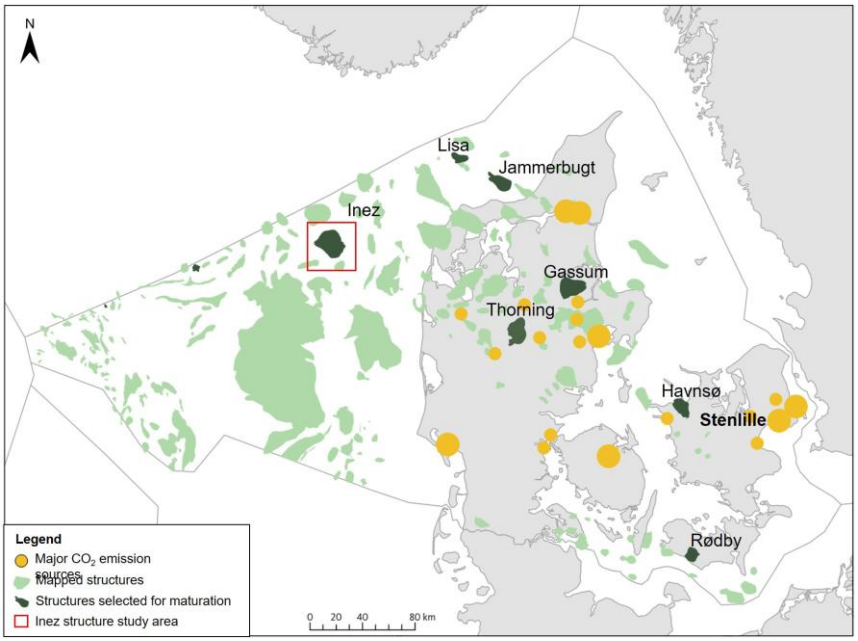

Figure 1.1. *Map showing Danish subsurface structures potentially suited for geological CO_2 storage. Named structures are being matured in feasibility studies by GEUS. The Inez structure is the focus of the current study. Yellow dots denote major CO_2 point sources. Modified from Hjelm et al. (2020).*

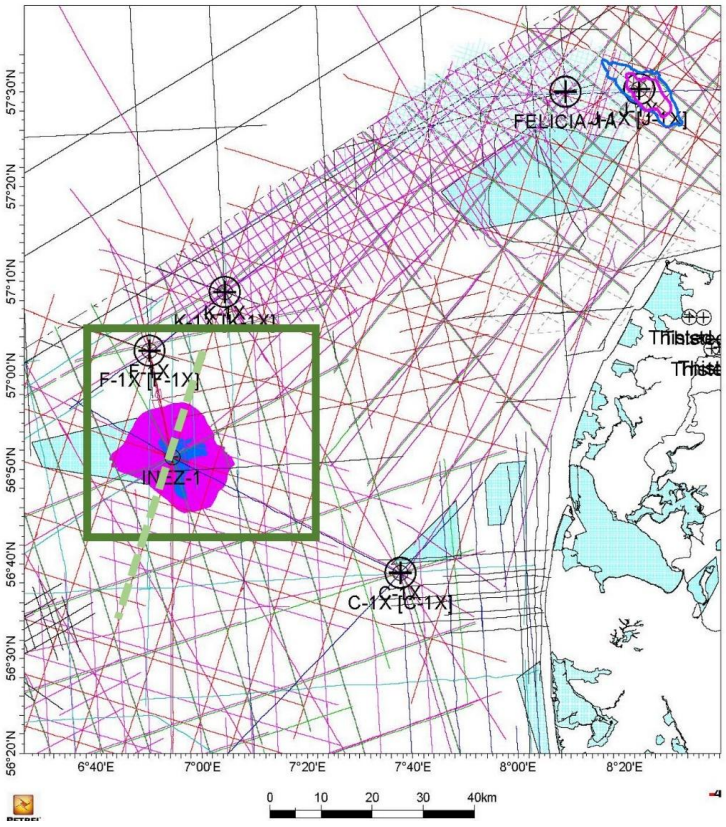

Figure 1.2. *Map with seismic data and wells interpreted around the Inez structure. The structure is outlined by pink and dark-blue areas that denotes the mapped closures at the top of the Haldager Sand Formation (dark-blue) and the Gassum Formation (pink). Light-blue areas denote Natura2000 areas. Green box indicates the location of TWT time-depth map shown in figure 1.3. Hatched green line illustrates the location of the seismic transect shown in figure 1.4.*

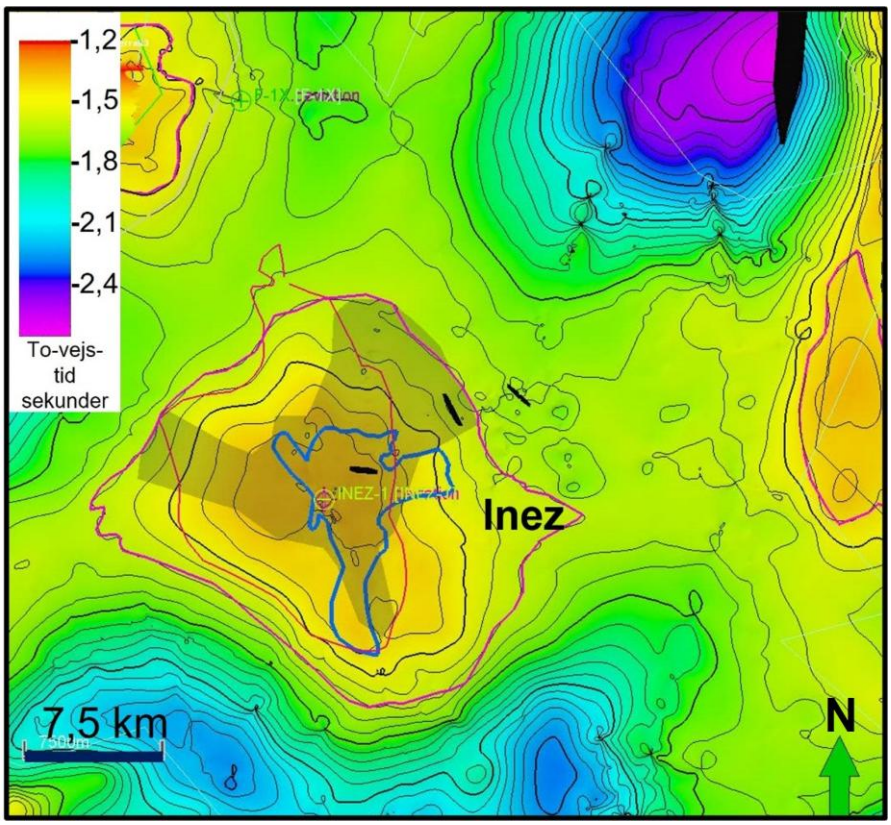

Figure 1.3. *TWT depth map to the top Gassum surface showing a well-defined roughly 0.2 s high four-way closure outlined by the pink curve. Shaded area indicates the densely faulted part of the Gassum Fm. The blue curve denotes the closure at top Haldager Sand level. Red curve outlines the closure at top Skagerrak level comprising the two secondary reservoir intervals. Based partly on TGS and Danpec A/S data.*

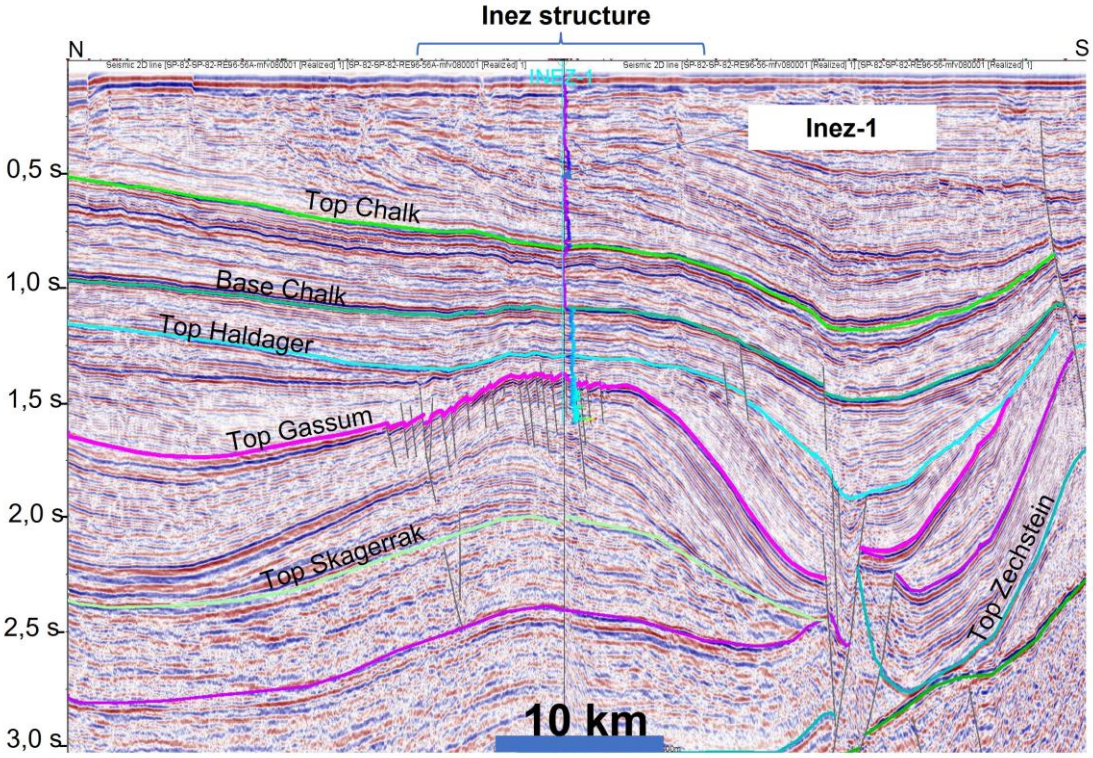

Figure 1.4. *Seismic section across the Inez structure and the Inez-1 well illustrating the structural and seismic stratigraphic geometry. Depth indicated in TWT. Location shown in figure 1.2 Composite line SP-82-RE96-56A & SP-82-RE96-56. Data Courtesy of TGS and Danpec A/S.*

2. Introduction

Sedimentary aquifers are well suited for CO_2 storage and form one of the most important means for lowering anthropogenic CO_2 emissions to the atmosphere (IPCC 2022). The Danish sedimentary storage potential is generally considered very high due to the widespread presence of porous aquifers sealed by tight, shaley formations (Frykman et al. 2009; Hjelm et al. 2020. In addition, large subsurface structures occur across much of Denmark including in the offshore areas (Fig. 1.1). In combination with reservoir and seal rocks, such structures may work to trap and permanently store CO_2 in the subsurface. Subsurface aquifers overlain by tight cap rocks (reservoir/seal pairs) exist underneath most of the Danish North Sea (Mathiesen et al. 2022). They vary in age and composition depending on their tectonic setting. The highest number of reservoir/seal pairs exists in the Norwegian–Danish Basin including its offshore part in the North Sea (Mathiesen et al. 2022). The North Sea part of the Norwegian–Danish Basin has been investigated since the 1960'es in the quest for hydrocarbons, but (virtually) lacks a petroleum system. Discovered hydrocarbon fields farthest west derive from long-distance migration into Paleogene aquifers (Hamberg et al. 2007), while *in situ* generated thermogenic hydrocarbons and their accumulation virtually lacks. Apart from local Paleogene sandstones with hydrocarbons, aquifers are therefore saline and hold the advantage over oil or gas charged aquifers that injected CO_2 will not displace hydrocarbons with the risk of their leakage. Moreover, saline aquifers are likely to be under hydrostatic pressure due to the moderate Neogene denudation of the region (Japsen et al. 2007).

The Inez structure located around 50 km off the coast of Jutland is one of the larger structures in the Danish part of the Danish-Norwegian Basin (Fig. 1.2). It was drilled by Chevron in 1977 in their pursuit for hydrocarbons, but the well and the structure was water-bearing. The well together with seismic data crossing the well site and covering the structure in an open grid has enabled a first assessment of its storage potential presented in this report.

3. Geological setting

The Inez structure is situated in the Norwegian–Danish Basin in a depression in the Top pre-Zechstein surface bound by extensional faults in the east (Fig. 3.1). The depression is separated from the Hurup Plateau by a 25 km wide zone characterized by intense halokinetic activity and deformation. To the north, the depression borders the Norwegian Farsund Basin, and to the south grades into the Horn Graben that intersects the Ringkøbing–Fyn High.

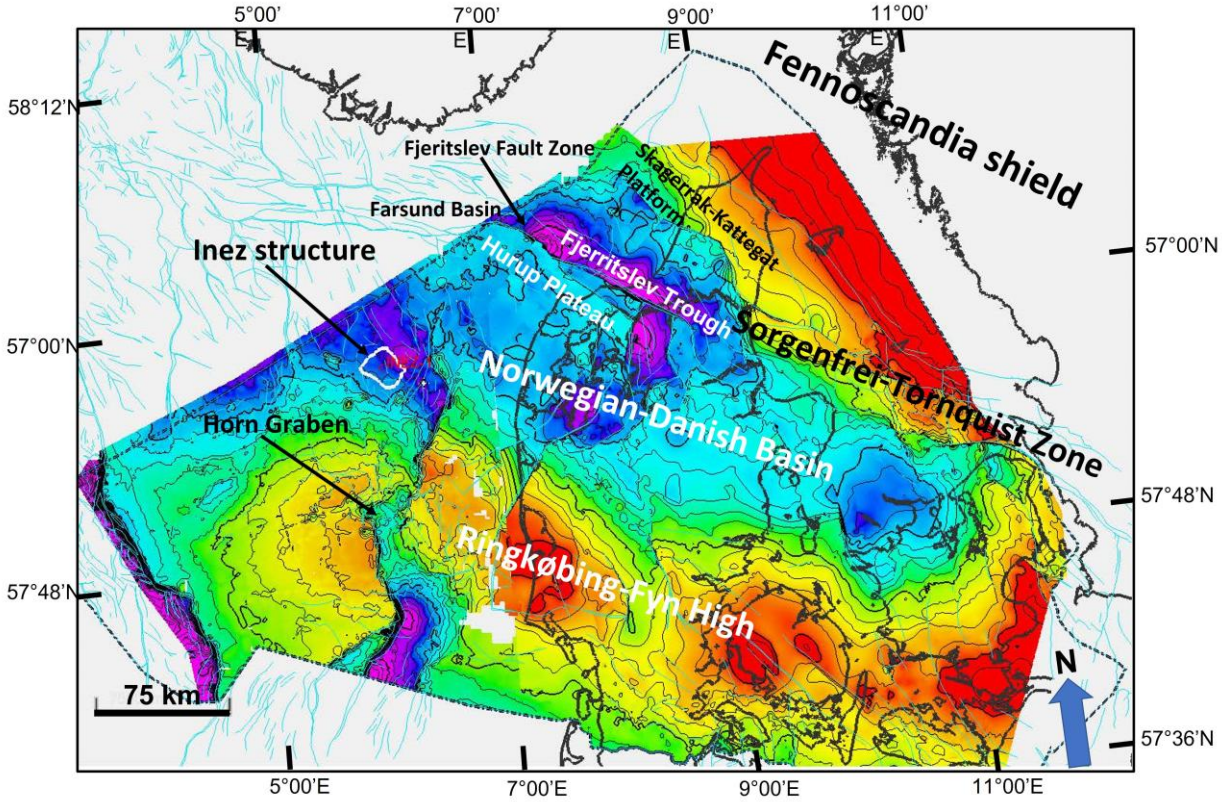

Figure 3.1. *Regional structural setting shown on a Top pre-Zechstein TWT depth map. Structural highs indicated by yellow to red colours while blue to pink colours outline depressions. The Inez structure is located in a depression in the Norwegian–Danish Basin delineating the northward extension of the Horn Graben.*

Rifting in Skagerrak and the northern North Sea occurred regionally in Carboniferous to Early Permian times and resumed more locally in the Triassic Horn Graben (Vejbæk, 1997). Triassic extension also affected the Fjerritslev Trough in the form of right-lateral transtension across the Sorgenfrei-Tornquist Zone (Phillips et al., 2018; Fyhn et al. 2022). Late Palaeozoic rifting was associated with volcanism, fluvial and aeolian-dominated dessert deposition, while subsequent Late Permian thermal relaxation and subsidence led to marine transgression and the accumulation of extensive Zechstein evaporites in a hot and dry climate over most of the Norwegian–Danish Basin (Michelsen & Nielsen, 1991; 1993; Stemmerik et al. 2000). During most of the Triassic, a continental, typically hot and dry/semi-dry environment existed (McKie 2014). Fluvial-dominated, red-bed deposition established in the earliest Triassic and a thick package developed covering the entire basin [Fig. 3.2] (Bertelsen 1980). During most of the Triassic, the western Ringkøbing–Fyn High acted as a low-relief barrier between the western Norwegian-Danish and the North German basins. Sediments in the western Norwegian–Danish Basin were therefore primarily sourced from the Scandinavian craton north and northwest of the basin (Bertelsen 1980; Olivarius et al. 2016; Olivarius et al. 2022). Alluvial fans fringed the craton and graded into

braid plains in the basin during the Early and Middle Triassic. This led to deposition of the sand-prone Skagerrak Fm. Extension renewed and subsidence intensified in the Late Triassic. Increased Late Triassic subsidence led to playa, shallow lake and sabkha deposition over the basin centre (Oddesund Fm) and restricted fluvial deposition to mostly along the basin margin (Skagerrak Fm) (Bertelsen 1980).

In the onshore, Triassic extension triggered differential salt movement (Bertelsen 1980). Offshore, the greater Inez region is located in a half-graben-like depression bound by faults to the east. The faults follow the trend of the Horn Graben but typically has moderate offset masked by hangingwall salt wedges and salt drapes, diapirs and pillows above the fault. While deep-seated extension was taken up by salt mobilization leaving the directly overlying Mesozoic unfaulted, Middle and Upper Triassic thickness variations document the contemporaneous timing of faulting. Hence, similar to the onshore, Triassic extension also triggered salt mobilization in the offshore. Salt movement continued throughout Mesozoic time and into the Cenozoic.

A restricted connection to the Tethys existed periodically in the Late Triassic (Bertelsen 1980; McKie & Williams 2009), which developed into a more permanent connection during Rhaetian time. As climate became more humid during the Rhaetian and Hettangian, deltas developed along the northern and north-western fringe of the basin associated with deposition of the sandstone-dominated Gassum Fm (Nielsen 2003). Transgression continued during the Early Jurassic and the basin became subject to open marine deposition and the development of the shaly Fjerritslev Fm (Michelsen et al. 2003). The Fjerritslev Fm also contains thinner sand interludes (Nielsen 2003; Vosgerau et al. 2016).

Later, in the Early and Middle Jurassic, the western and southern Norwegian–Danish Basin – including the Inez area - was uplifted and subject to erosion (Nielsen 2003) due partly to rifting and formation of the Central Graben in the west. The mid-Cimmerian unconformity record this event. Uplift over the north-eastern part of the basin located along the Sorgenfrei-Tornquist Zone was limited and the sand-prone Haldager Sand Fm formed during Middle Jurassic times (Nielsen 2003). The formation thins south-westwards and is typically no more than a few meters to tens of meters thick away from the Sorgenfrei-Tornquist Zone and lacks on the Ringkøbing–Fyn High and to the south.

As subsidence resumed in southwestern Skagerrak in the Late Jurassic, the Haldager Sand Fm became buried by typically muddy Upper Jurassic and Lower Cretaceous open-marine deposits. Sedimentation changed from clastic to carbonate deposition towards the Late Cretaceous and the Chalk Group developed as a thick Upper Cretaceous and Lower Paleocene blanket over much of western Europe (Surlyk et al. 2003). Late Cretaceous and Palaeogene inversion and local uplift/erosion affected part of the Central Graben and Sorgenfrei-Tornquist Zone (Mogensen & Jensen, 1994; Vejbæk & Andersen 2002; van Buchen et al. 2017). Meanwhile, the Danish portion of the Norwegian–Danish Basin away from the Sorgenfrei-Tornquist Zone was subsiding and tilting towards the west. This lasted until middle Neogene time when deposition ended through regional uplift and erosion (Japsen et al. 2007). The Norwegian–Danish Basin experienced between 0 and roughly 1 km of uplift and erosion. 300-500 m of Neogene erosion is suggested in the Inez area by consistent shale and chalk compaction and apatite fission track studies (Japsen et al. 2007). The lower estimate fits best with the thickness, truncation- and internal reflection pattern of the upper Neogene preserved west of Inez and imaged seismically.

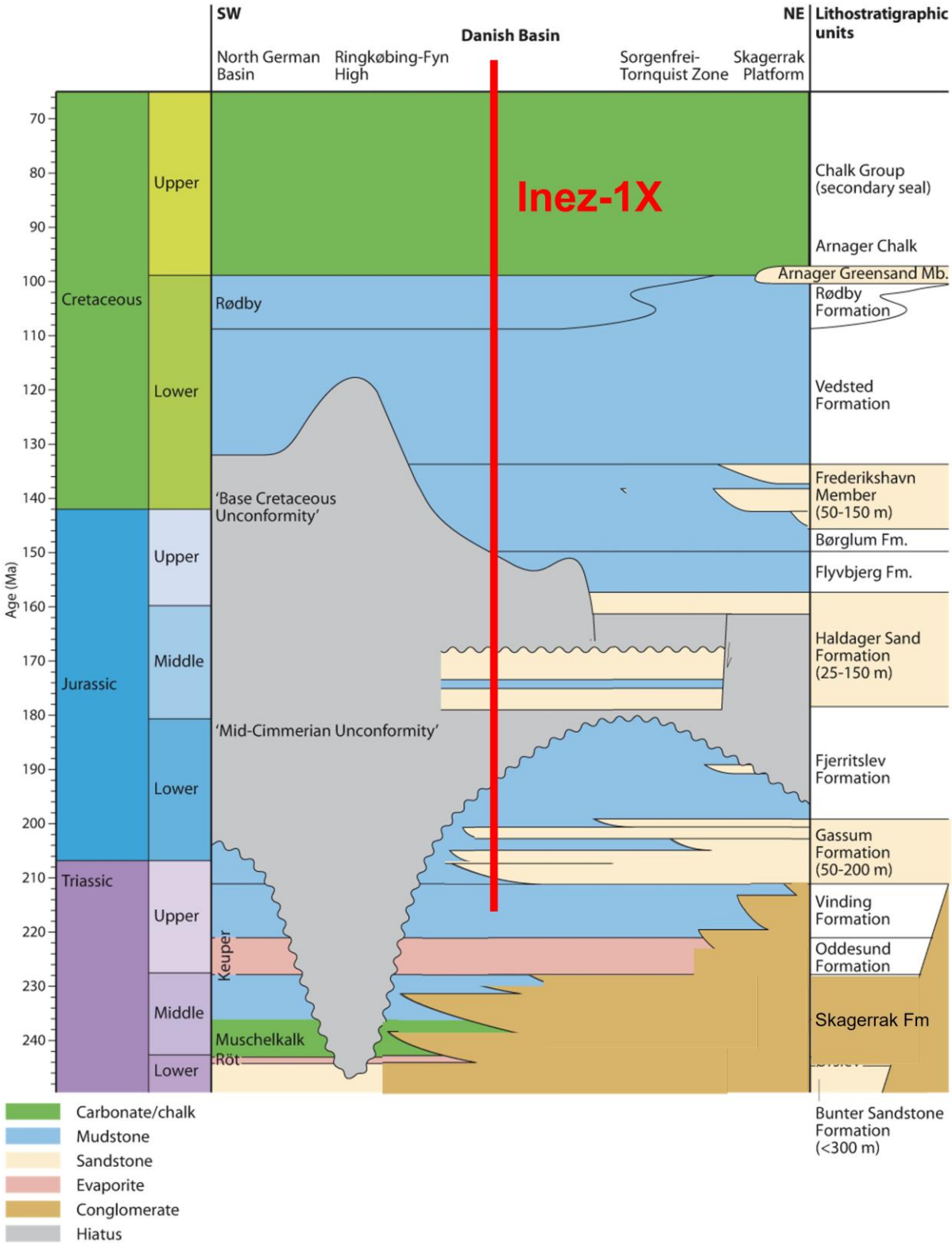

Figure 3.2. *Simplified Mesozoic stratigraphy of the Danish Basin of the North Sea area outside Central Graben modified from Mathiesen et al. (2022) and Nielsen (2003).*

4. Database

4.1 Seismic data

The Inez structure and the investigated area surrounding it are covered by 1577 kilometers of vintage 2-D seismic data forming an uneven seismic grid, the bulk of which was collected by the oil and gas exploration industry in the 1980s and earlier (Fig. 1.2). supplemented by a few additional lines acquired by academia during the 1990s. The latter of which is of moderate quality and has virtually no resolution of the pre-Cretaceous. TGS and Danpec A/S in the 1990s reprocessed 947 km of the 1980s industry data kindly made available for the Inez study. These reprocessed data and the remaining industrial seismic data acquired in the 1980s are of good to reasonable quality, while the older industrial data has poor resolution. Eighteen of the available seismic lines tie to the Inez well. The lines are of variable vintages and has been acquired in a starshaped pattern centring on the drilled crest of the Inez structure. While this provides a dense 2-D seismic coverage over the apex of the Inez structure, it results in a less dense and unsystematic seismic coverage of the more marginal part of the structure. The seismic data were acquired in various surveys using different equipment and processing techniques. Consequently, their quality varies and mis-ties up to a few tens of milliseconds occur between the seismic sections.

4.2 Well data

The Inez structure was tested in 1977 by the Inez-1 well. The well was drilled by Chevron as operator on behalf of DUC in their pursuit for hydrocarbons but was water-bearing (apart from faint traces of oil in a lower Fjerritslev Fm sandstone interbed) (Chevron 1978). Inez-1 TD'ed in 1949 m b. msl (total depth & below mean sea level, respectively) depth in the Upper Triassic. Available petrophysical logs comprise calliper, gamma ray, sonic, resistivity, neutron porosity and density. No conventional cores were cut but 56 plugs were retrieved from between 1095 m and 1945 m depth b. msl. No data on mechanical properties, in situ stress, leak off tests or rock failure data were acquired in the Inez-1 well.

Around 22 km north of the Inez-1, the exploration well F-1 was drilled in 1968 by Gulf on behalf of DUC with a TD 2385 m b. msl in the Upper Triassic to test the hydrocarbon potential of the area. Roughly 34 km north-northwest of Inez-1, the exploration well K-1 well was drilled in 1970 by California Oil Company on behalf of DUC and has TD at 2254 m b. msl in the Upper Triassic. Ties to the two wells provide additional support to the stratigraphic interpretation of the Upper Triassic through the Cenozoic. Farther northeast, the exploration well Felicia-1 was drilled by Statoil in 1987 to a TD of 5290 m b. msl flooring in the Permian Rotliegende Group to test the hydrocarbon potential of the area. The well was water-bearing, but two cores were cut from the Permian section in the Felicia well (Statoil 1988). Tie with Felicia-1 has been used to constrain the age of the Middle Triassic and older succession. As argued below, the Lower–Middle Triassic reservoir rocks in Felicia-1 have had a maximum burial roughly compatible with the same stratigraphic interval in the Inez structure. The drilled Lower–Middle Triassic sandstones in Felicia-1 have therefore been used as analogue for the reservoir potential of the undrilled succession beneath 1945 m b. msl in the Inez area. The four wells have been tied to seismic data and comprise the primary well control to the evaluation of the Inez structure.

5. Methods

5.1 Seismic interpretation and well-ties

The Inez structure is evaluated based on conventional analysis of all available 2-D seismic data over the greater Inez area (Fig. 1.2). Interpreted seismic horizons and units were tied to wells to build a stratigraphic framework (Fig. 5.1.1). Seismic horizons, seismic successions/facies are interpreted, using onlap, downlap, truncation, seismic attributes and successions identified by different seismic facies. The horizons are essentially sequence stratigraphic/chronostratigraphic surfaces but can in this limited area be regarded as near base/top of formations, with horizon names similar to the formations tied from the wells. The seismic interpretation and well-ties with synthetic seismograms are performed on a workstation with Petrel (2022) software.

Eight surfaces were mapped systematically over the area due to their importance for defining reservoir-seal pairs, structural closures, and for determining the geological evolution of the area. These are from oldest to youngest the (1) Top pre-Zechstein, (2) Top Zechstein, (3) Top Bunter Sandstone, (4) Top Skagerrak, (5) Top Gassum), (6) Top Haldager Sandstone, (7) Base Chalk, and (8) Top Chalk. To aid analysis of the tectonic and depositional development of the Inez area, approximate chronostratigraphic ages were assigned based on biostratigraphy in the Inez-1 well and on regional considerations and biostratigraphy from the Felicia-1 well for the surfaces not intersected in the well.

At the same time, faults, salt structures and folds were mapped together with internal lapping and thickness patterns, and a structural and tectonic analysis was performed by integrating the structural observations with the chronostratigraphic framework permitted by the well ties.

The storage complex including identification of reservoir-seal pairs was investigated and evaluated based on the structural and stratigraphic analysis and based on the available well data. Primary weight was put on the data derived from the Inez-1 well for the reservoir-seal pairs intersected in the well, while the Felicia-1 well provided information on the deeper Skagerrak Fm-Oddesund Fm reservoir-seal pair not intersected in Inez-1.

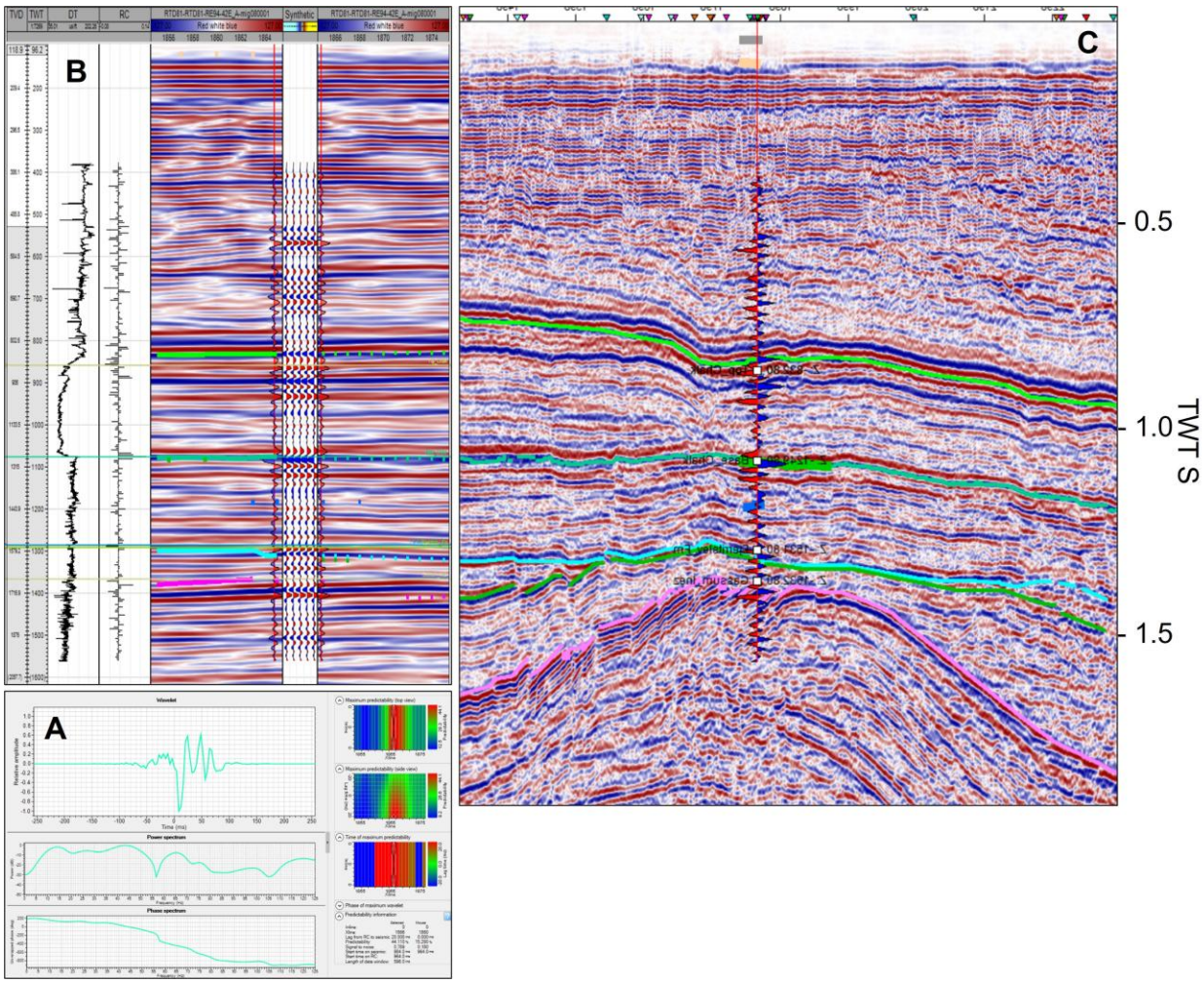

Figure 5.1.1. *A deterministic wavelet along the Inez-1 borehole was extracted and used for forward modeling and generation of a synthetic seismogram (A). A window of 10 traces on both sides of the borehole are used to predict the best possible wavelet with maximum correlation. Wavelet convolved with the spike function generated along the borehole using sonic log generates a synthetic seismogram for Inez-1 which overall shows a good fit with the existing seismic intersecting the well (B). The stratigraphy picked in the Inez-1 well fits well with the seismically picked stratigraphic surfaces (C). Tie with line RTD81-RE94-42E. Data Courtesy of TGS and Danpec A/S.*

5.2 Seismic time to depth conversion

Prior to interpretation of different seismic horizons, a detailed 1D forward modeling was performed for Inez-1. Sonic log in this well was calibrated and seismic wavelet was extracted along the borehole and the intersecting seismic line. Reflection coefficient series for the well (derived from the product of density and p-wave velocity within the borehole) was convolved with the extracted seismic wavelet to generate a synthetic seismogram that was used to derive time depth relationship between Inez-1 and intersecting seismic line. Table 5.2.1 summarizes the time depth relationship for Inez-1.

A quadratic relationship between time and depth was derived for Inez-1 and used for converting structure maps from time domain into depth (Fig. 5.2.1). Depth structure maps were back interpolated to compensate for the difference in actual depth and the predicted depth along the Inez-1.

Table 5.2.1. *Time-depth relationship and acoustic velocities in Inez-1*

Well name	MD (m)	TWT (ms)	Average velocity (m/s)	Interval velocity (ms/s)
Inez-1	35.00	0.00		1952.38
	404.00	378.00	1951.32	2000.00
	431.00	405.00	1954.57	2000.00
	462.00	436.00	1957.80	2000.00
	492.00	466.00	1960.52	2066.67
	523.00	496.00	1966.94	1935.48
	553.00	527.00	1965.09	1937.50
	584.00	559.00	1963.51	2068.97
	614.00	588.00	1968.71	2066.67
	645.00	618.00	1973.46	2142.86
	675.00	646.00	1980.80	2296.30
	706.00	673.00	1993.46	2142.86
	736.00	701.00	1999.43	2384.62
	767.00	727.00	2013.20	2222.22
	797.00	754.00	2020.69	2137.93
	828.00	783.00	2025.03	2142.86
	858.00	811.00	2029.10	2137.93
	889.00	840.00	2032.86	2857.14
	919.00	861.00	2052.96	3444.44
	950.00	879.00	2081.46	3157.89
	980.00	898.00	2104.23	3444.44
	1011.00	916.00	2130.57	4000.00
	1041.00	931.00	2160.69	4133.33
	1072.00	946.00	2191.97	4000.00
	1102.00	961.00	2220.19	4133.33
	1133.00	976.00	2249.59	4000.00
	1163.00	991.00	2276.08	4428.57
	1194.00	1005.00	2306.07	4000.00
	1224.00	1020.00	2330.98	3750.00
	1254.00	1036.00	2352.90	3875.00
	1285.00	1052.00	2376.05	2222.22
	1315.00	1079.00	2372.20	5166.67
	1346.00	1091.00	2402.93	2500.00
	1376.00	1115.00	2405.02	5636.36
	1407.00	1126.00	2436.59	1666.67
	1437.00	1162.00	2412.74	2583.33
	1468.00	1186.00	2416.19	2608.70
	1498.00	1209.00	2419.85	5166.67
	1529.00	1221.00	2446.85	1764.71
	1559.00	1255.00	2428.37	2583.33
	1590.00	1279.00	2431.27	2727.27

	1620.00	1301.00	2436.28	2583.33
	1651.00	1325.00	2438.94	2608.70
	1681.00	1348.00	2441.84	2818.18
	1712.00	1370.00	2447.88	2727.27
	1742.00	1392.00	2452.30	3100.00
	1773.00	1412.00	2461.47	3000.00
	1803.00	1432.00	2468.99	3100.00
	1834.00	1452.00	2477.69	3000.00
	1864.00	1472.00	2484.78	3263.16
	1895.00	1491.00	2494.70	3157.89
	1925.00	1510.00	2503.05	3263.16
	1956.00	1529.00	2512.49	3157.89
	1986.00	1548.00	2520.41	3444.44
	2017.00	1566.00	2531.03	

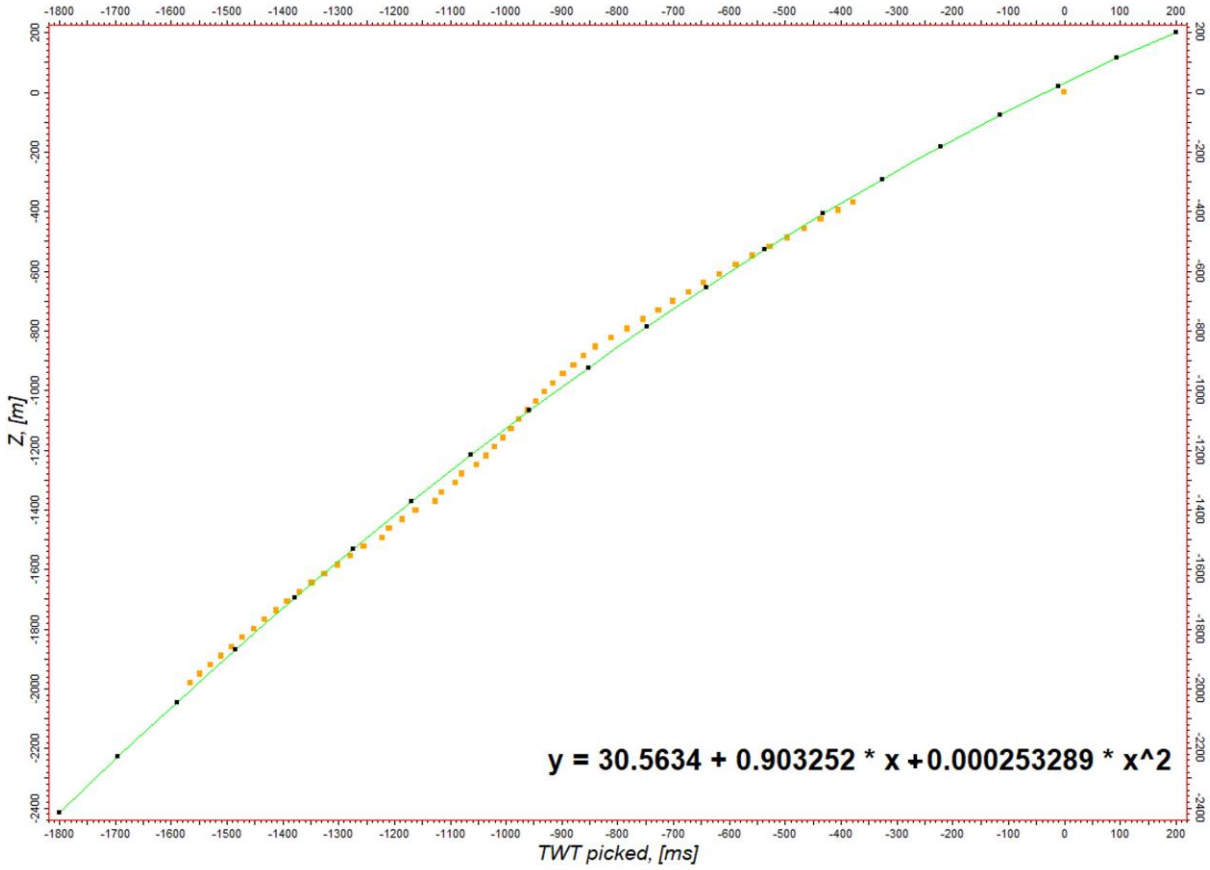

Figure 5.2.1. *Time-depth relationship between Inez-1 and seismic. Yellow dots represent the actual depth along the borehole whereas the black dots represent the predicted depths. Black dots are used to generate a polynomial function (y = 30.5634 + 0.903252 * x - 0.000253289 * x^2). There is a good fit between actual depth and predicted depths. However, difference between actual and predicted depths is calculated for each depth map and is compensated.*

5.3 Investigation of reservoir and seal

The reservoir characteristics presented below and in Chapter 7 are derived mainly from the obtained wireline logs but cross-checked against descriptions of cuttings and sidewall cores. Potential reservoir units were identified on wireline logs by their low formation resistivity, low formation density and a natural radioactivity as seen by low GR log readings and in cuttings containing sand-sized quartz grains. Reservoir parameters were evaluated based on well data with emphasis on data from the Inez-1. A sandstone is defined on the petrophysical data as a rock having < 50% volume of shale, and a reservoir sandstone has estimated effective porosity (PHIE) of > 0.1. The volume of shale is estimated based on a combination of the gamma ray, deep resistivity, density and neutron porosity logs, while the effective porosity is calculated based on the volume of shale along with the density and neutron porosity logs. The permeability is based on an in-house established data relation between porosity and permeability. As there are no cores from relevant reservoir intervals and therefore no conventional core analysis in the offshore part of the Norwegian–Danish Basin, the permeability is based on a best fit relation between measured core porosities to measured permeabilities from onshore Denmark.

Seal thickness and grain-sizes were similarly evaluated based on petrophysical logs. Mudstone sections that will act as seal were identified from wireline logs by having high formation resistivity, high formation density and having high natural radioactivity reflected in high GR log readings. In addition, information on the regional composition such as total organic carbon (TOC) content and clay mineralogy of the potential sealing units were included in the seal analysis together with seal quality analysis performed on these units from other Danish wells.

A mud gas log from the Inez-1 well was available as a hard copy in the completion report (Chevron 1978). Data can be included in seal integrity studies by evaluating the gas type and concentrations in the reservoir and seal sections. See Petersen et al. (2022) and Petersen and Smit (2023) for details.

5.4 Storage capacity modelling

The storage capacity of reservoir units with buoyant trapping is estimated via this equation:

$$SC = GRV * N{:}G * \varphi * \rho_{CO2R} * S(Eff.)$$

Where:

SC	Storage Capacity
GRV	Gross Rock Volume is confined within the upper and low boundary of the gross reservoir interval and above of the deepest closing contour from where spillage from a trap will occur
N/G	Average net to gross reservoir ratio of aquifer across the trap
φ	Average effective reservoir porosity of aquifer within trap
ρ_{CO2R}	The average CO_2 density at Reservoir conditions across all of trap.
$S(Eff.)$	Storage efficiency factor relates to the fraction of the available pore volume that can store CO_2 within the trap (GRV). This fraction depends on the size of storage domain, heterogeneity of formation, permeability, porosity, compartmentalization and compressibility, but is also strongly influenced by different well designs and injection schemes (Wang et al. 2013).

To address the uncertainties associated with seismic data quality / density, interpretation and seismic well tie, depth conversion challenges, mapping, reservoir parameters assessment and fluid parameter assumptions in the reservoir, a simple Monte Carlo methodology has been applied. Ranges of each of the four input parameters (GRV, N/G, φ and ρ_{CO2R}) have been chosen to reflect parameter uncertainty and distribution modelled utilizing a simple Monte Carlo simulation tool built in MS Excel®. To achieve stable and adequate statistical representation of both input distribution and result output, 10.000 trials are calculated for each simulation. The methodology is simplistic and does not incorporate e.g. correlations of input parameters. However, for the purpose of estimating reliable screening volumes, the methodology is considered relevant and adequate. The method is used for the calculations in Chapter 8.

6. Results

6.1 Local Stratigraphy

The Inez area contains a thick accumulation of Palaeozoic through Cenozoic deposits (Fig. 3.2). The Inez-1 well floors in the Upper Triassic and only intersects part of this succession. The youngest section intersected consists of almost 800 m of Cenozoic, dominantly southwards prograding siliciclastic deposits (Figs. 6.1.1 & 6.1.2). This unit overlies 417 m of the Paleocene to Upper Cretaceous Chalk Group that rests on 145 m, Lower Cretaceous claystone-dominated Vedsted Fm. The underlying Upper Jurassic section (excl. Haldager Sand Fm) is 129 m thick and consists of Frederikshavn Fm (83 m) and Børglum Fm (46m) [Fig. 6.1.3]. These two formations are claystone-dominated in Inez-1 apart from a minor mudstone interval in the upper part. The Børglum Fm rests on 9 m sandy Haldager Sand Fm presumably of Kimmeridgian age that caps the mid-Jurassic mid-Cimmerian unconformity according to Nielsen and Japsen (1991). .

Erosion of the underlying Lower Jurassic Fjerritslev Fm is indicated by seismic reflector truncation over the Inez structure, particularly over the crest and western flank. The claystone-dominated Fjerritslev Fm as defined in this study is 127 m thick in Inez-1 over the crest of the structure but thickens down the eastern, northern, and southern flank. It is dated as Hettangian to Sinemurian in age in Inez-1 but probably includes younger Lower Jurassic strata over the southern, eastern, and northern flanks of the Inez structure with less mid-Cimmerian truncation. The underlying Gassum Fm met in 1659 m b. msl (1694 m b. kb) defined here as the underlying, continuous Rhaetian to lowermost Hettangian reservoir sand-prone unit measures 148 m in thickness and was deposited in a marginal marine to non-marine setting. This is a redefinition of the Gassum Fm compared to that of Nielsen and Japsen (1991) that places the top of the Gassum Fm at 1633 b. msl on the basis of the first downwards occurrence of Hettangian sand. However, this only ~2 m thick sand bed is underlined by 24 m of Hettangian claystones that resemble the Fjerritslev Fm, and we here attribute the sand bed to the Fjerritslev Fm comparable to coarse-grained interludes observed in the lower part of the Fjerritslev Fm elsewhere (Nielsen 2003; Vosgerau et al. (2016). Nielsen and Japsen (1991) follows Bertelsen (1980) and picks the base of the Gassum Fm in Inez-1 at 1704 m b. msl and interpret 245 m of underlying Skagerrak Fm. However, the underlying Rhaetian section down to 1809 m b. msl (1844 m b kb) is also marine influenced, sand-dominated and does not distinguish markedly from the overlying deposits and we here include it within the Gassum Fm for practical reasons and on similar grounds as the redefined Triassic stratigraphy in the J-1 presented by Fyhn et al. (2023).

The Gassum Fm also seems to thicken along the southern flank of the Inez structure. We also note a change in seismic facies of the Gassum Fm interval over the Inez structure. To the north, the Gassum Fm interval is characterized by relatively discontinuous and low- to intermediate-amplitude reflections, while over the southern half, it is characterized by fairly strong, continuous reflections (Fig. 6.1.4). The change in seismic facies is interpreted to reflect a change from a more proximal, possibly more fluvially influenced facies in the north to a more distal, probably more marine influenced depositional facies – and thus continuous seismic facies - over the southern half, possibly with carbonate interbeds (typical for the Vinding Fm with which the Gassum Fm intercalates) resulting in the strong reflection amplitudes. Towards the base of Inez-1, the lower Rhaetian succession becomes increasingly evaporitic, contains limestone interbeds, brick-red mudstone interludes, few arkosic sandstones and has very few marine indicators. Compared with the roughly time-equivallent interval in the Felicia-1 and J-1 wells, this suggests a more landward depositional setting in line with the reconstruction of Bertelsen (1980) of the Late Triassic gross-depositional environment. While Bertelsen (1980) attributed this lower section to the Skagerrak Fm, we suggest that this is better considered as part of the Oddesund Fm or a proximal facies of the Vinding Fm. The well terminates in this unit and only seismic data tied with the distant Felicia-1 well provides some indications of the nature of the underlying section. The seismic facies of this lowermost section in Inez-1 is compatible with the underlying undrilled several hundred meters thick section. It is characterized by relatively continuous reflectors with intermediate to strong reflection amplitudes possibly corresponding to

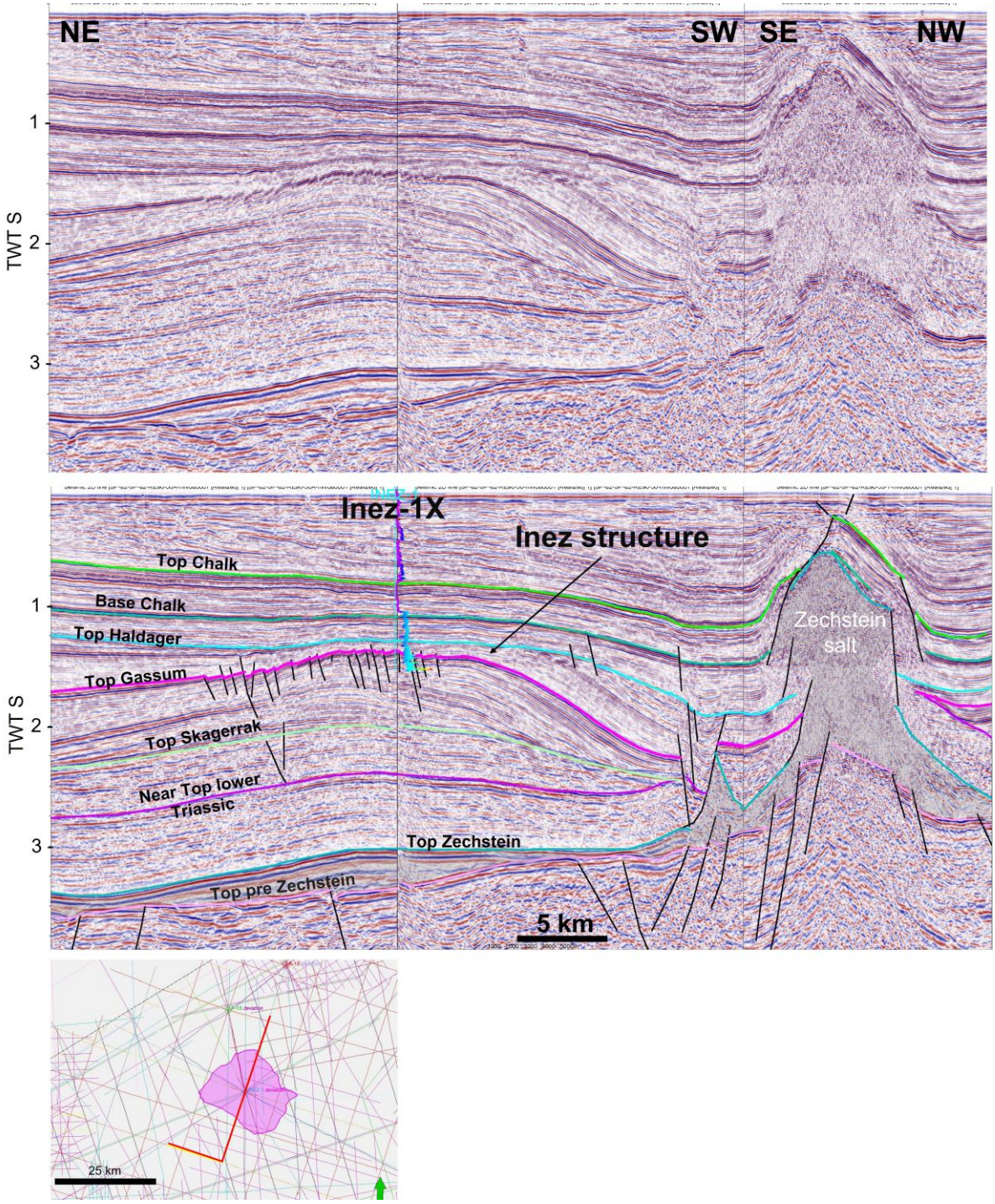

Figure 6.1.1. Composite s*eismic transect across the Inez structure and intersecting the Inez-1 well (uninterpreted and interpreted). The line illustrates the interpreted seismic stratigraphy in the greater Inez area. Salt diapirs evolvede on top of Top pre-Zechstein structural highs flank the Inez structure. The lense-shaped stratigraphic growth geometry formed in response to gradual salt withdravel and associated differential subsidence in the Inez area. Note that these thickness growth geometries primarily occurs above the Lower Triassic and are especially well-developed in the Upper Triassic (above the Skagerrak Fm) and in the Lower Jurassic situated between the Gassum and Haladager Sand fms. Only a subtle salt pillow underneath the Inez structure remains. Line location indicated by red line in the lower map. Composite line SP-82-RE96-56A & SP-82-RE96-56. Data Courtesy of TGS and Danpec A/S.*

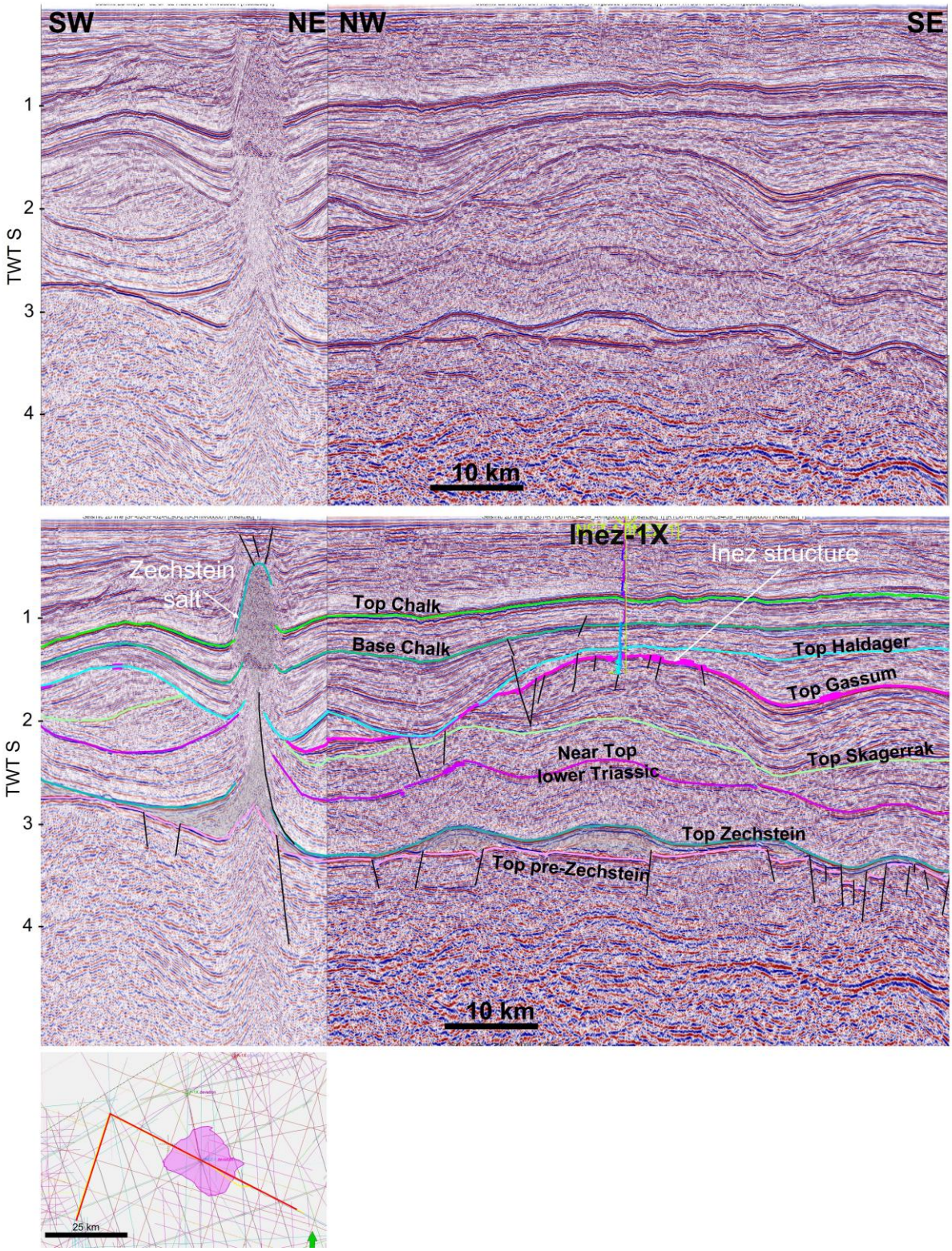

Figure 6.1.2. Composite s*eismic transect across the Inez structure and intersecting the Inez-1 well (uninterpreted and interpreted). The line illustrates the interpreted seismic stratigraphy in the greater Inez area and the complex stratigraphic thickness variations that were established in response to differential Zechstein salt movement as well as differential erosion along the mid-Cimerian unconformity underneath the light blue Near Top Haldager Sand Fm horizon. Line location indicated by red line in the lower map. Composite line SP-82-RE96-210-3 & RTD81-RE94-39. Data Courtesy of TGS and Danpec A/S.*

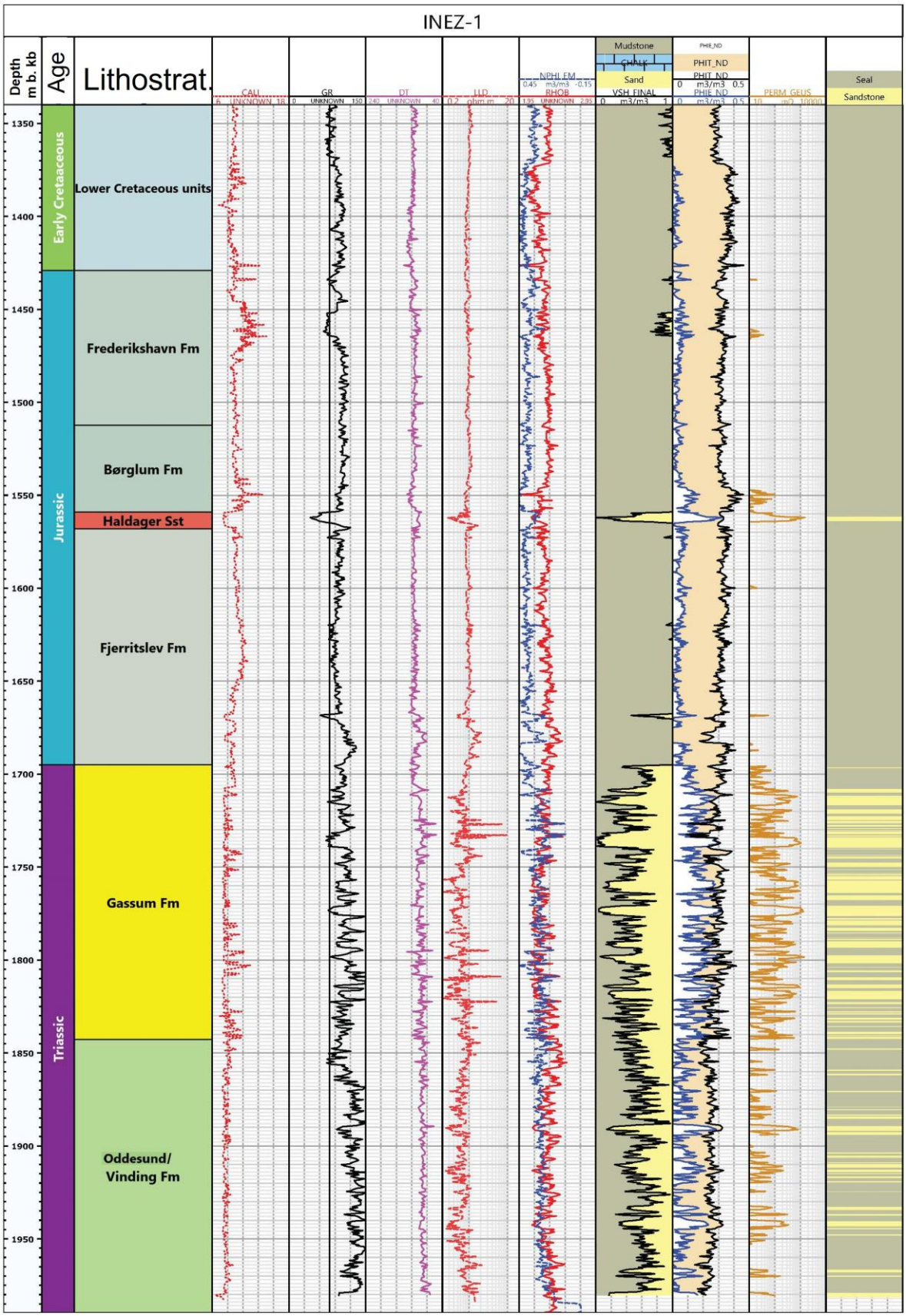

Figure 6.1.3. *Well stratigraphy, geoelectric logs and interpreted lithology and reservoir characteristics of the Inez-1 section Depth are indicated in meter below KB located at around 35 m above mean sea level.*

Oddesund Fm deposits with evaporite-rich interbeds. Beneath this section at around 2 seconds depth at Inez-1, amplitudes and continuities decrease. Long distance seismic correlation with Felicia-1 suggests that this roughly corresponds to the top of the Skagerrak Fm. The change from Oddesund Fm to Skagerrak Fm in the Felicia-1 well for instance marks a downward shift from typically muddy playa- and sabkha dominated deposition to more fluvial dominated deposition lithologically characterized by a very thick unit consisting of interbedded sand- and mudstones passing downwards to a more sand-dominated succession. The downwards change towards sandstone-dominated deposits may be marked by a continuous set of reflectors that chronostratigraphically corresponds to the top of the Bunter Sandstone Fm found in the Horn Graben and the North German Basin. The Triassic rests on salt-dominated Zechstein deposits. The salt probably caps Rotliegendes and older strata that are only poorly seismically resolved.

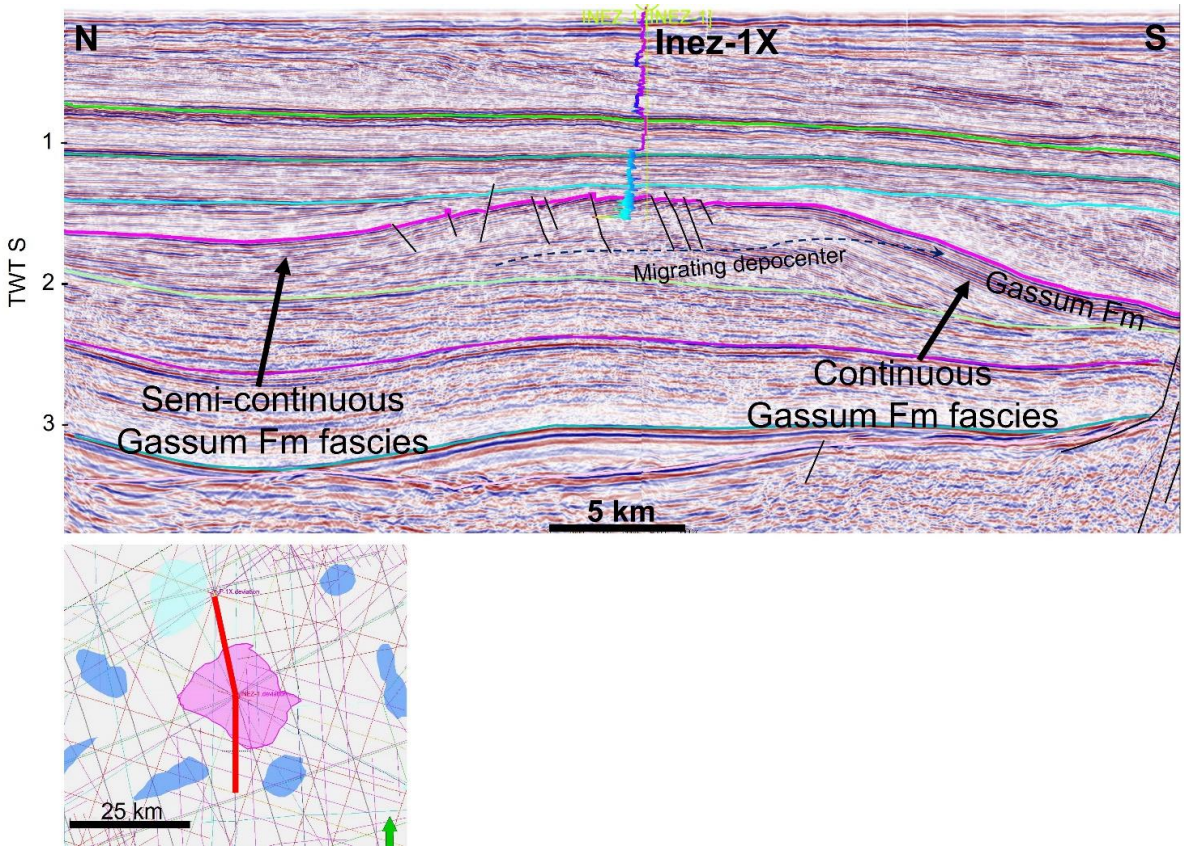

Figure 6.1.4. *Seismic transect illustrating the lateral migration of depocenter resulting from a migrating rim syncline. Rim synclines formed along the salt structures surrounding the Inez area (salt diapirs marked by dark blue polygons on map, large salt pillow with light blue polygon. Also note the variation in Gassum Fm seismic facies underneath pink horizon: in the north seismic facies is characterized by intermediate reflection amplitude and semi-continuous reflectors while the facies to the south is characterized by continuous, high-amplitude reflectors – a change possibly reflecting a higher marine influence towards the south. Composite line SP-82-RE96-82A-1 & SP-82-RE96-82-1. Data Courtesy of TGS and Danpec A/S.*

6.2 Structure

The Inez structure is a four-way closure on the Top Gassum, Skagerrak, Bunter Sandstone and Haldager Sand Fm levels (Figs. 6.2.1; 6.2.2) that outline a large turtle-back structure underlain by a small Zechstein salt pillow/salt lens (Fig. 6.1.2). The Inez structure is located in an area

surrounded by six salt diapirs/salt walls and a salt pillow (Fig. 6.2.3). Thickness variations and lapping patterns within especially the Middle Triassic to Lower Cretaceous indicate that the Inez structure formed due to evacuation of Zechstein salt in association with the development of the surrounding salt diapirs and pillow through a long and highly dynamic history of Zechstein salt motion. Salt mobilization initially resulted in the inflation of salt pillows along Inez associated with salt evacuation from neighbouring areas. With time, the salt pillows migrated, build up and eventually pierced the overlying stratigraphy generating salt diapirs/salt walls. During the salt evacuation, rim synclines formed and were filled with sediments. With time, the rim synclines migrated laterally causing gradual shifts in depocenters and on-lap within the Middle Triassic through Cretaceous. The Lower Triassic, time-equivalent to the Bunter Sand and Bunter Shale formations, drapes the Zechstein salt and is characterized by a uniform thickness. These units thus formed prior to the mobilization of Zechstein salt. Thickness variations and laterally migrating base laps (originally formed as onlaps) within the Middle Triassic record the onset of salt motion (Figs. 6.1.1; 6.1.2). Judging by the thickness variations and internal lapping pattern, differential salt movements continued and intensified throughout the Triassic, Jurassic and Early Cretaceous time, slowing during the Late Cretaceous but picking up again in Cenozoic time in narrow zones around the six diapirs that by then pierced through the Mesozoic and part of the Cenozoic succession. The Inez structure was virtually unaffected by this late-stage salt motion.

The Top pre-Zechstein surface is offset by faults underneath the diapirs (Fig. 6.1.1). Velocity pull-ups typically mask the offset, which may be in the order of a few hundred meters vertically. Smaller faults, both in length and heaves, offset the Top pre-Zechstein locally in the Inez area (Figs. 6.1.1; 6.1.2). The deep-seated faulting does not intersect the Zechstein evaporites. Elsewhere, shallow-seated growth faults within the Triassic and Jurassic sole out in Zechstein evaporites (Fig. 6.2.4). The deep-seated faults are interpreted to be associated with Triassic to Jurassic deep-seated extension coupled with the shallower faults through a Zechstein salt decollement. The moderate Triassic extension triggered salt motions, and the Top pre-Zechstein fault offsets acted as nucleation sites of salt structures. The uniform thickness of the time-equivalent to the Bunter Sandstone/Shale fms suggests that faulting primarily occurred from after the Early Triassic.

Initial salt motion commenced during the Middle Triassic deposition of the upper Skagerrak Fm that displays a lateral thickness variation and internal lapping pattern compatible with salt pillow growth south and east of Inez (Fig. 6.1.1). The Inez area was located in a broad rim syncline setting and Middle Triassic deposits (Skagerrak Fm) became thickly developed. Subsequently, during Oddesund Fm-time, salt migration expanded, and salt pillows started to form north, east and west of Inez in addition to continuing growing south of the structure (Figs. 6.1.1; 6.1.2; 6.2.4). The thickness variation and internal lapping pattern suggest that the salt pillows build up and narrowed and that the rim-syncline(s) migrated laterally away from the present crest of the Inez structure; a process continuing throughout Late Triassic and Early Jurassic time. Consequently, the stratigraphy corresponding to the Vinding, Gassum and Fjerritslev formations are thickest developed along the flanks of the Inez structure (Fig. 6.2.3). Even so, the sand-prone Gassum Fm, as defined here, are around 148 m thick in the Inez-1 well intersecting the apex of the structure.

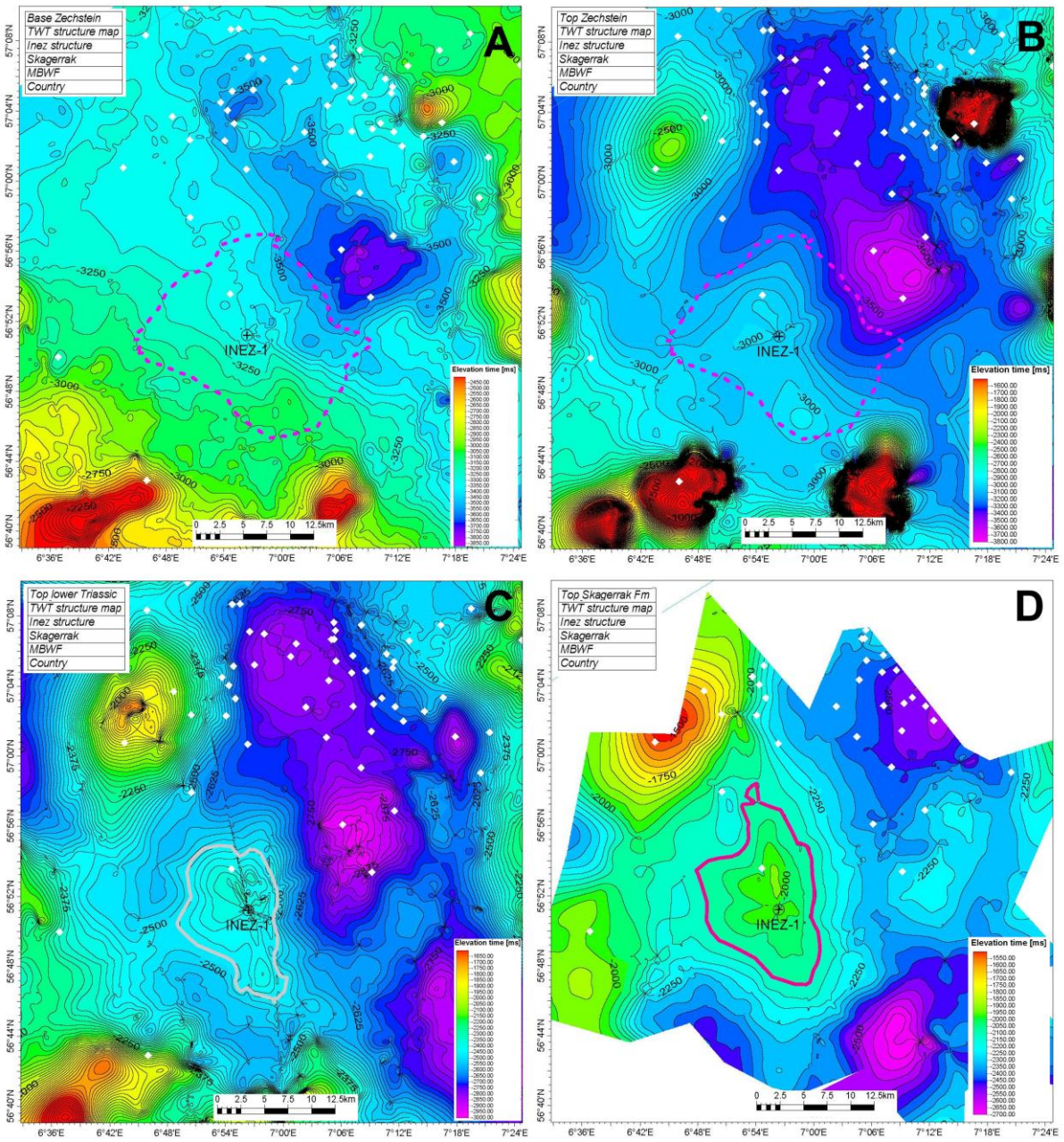

Figure 6.2.1. *Seismic TWT structure depth maps with a 50 ms contour interval.* ***A*** *Base Zechstein;* ***B*** *Top Zechstein;* ***C*** *near-Top Lower Triassic;* ***D*** *near top Middle Triassic (Top Skagerrak Fm);* ***E*** *Top Gassum Fm (Near-top Triassic);* ***F*** *near top Haldager Sand Fm (Near-top Lower Jurassic);* ***G*** *Base Chalk (intra-mid-Cretaceous);* ***H*** *Top Chalk (intra Paleocene). Structural closures are indicated with bold contour lines at reservoir levels, while Top Gassum closure is indicated with dashed signature as geo reference at non-reservoir levels. Based partly on TGS and Danpec A/S data.*

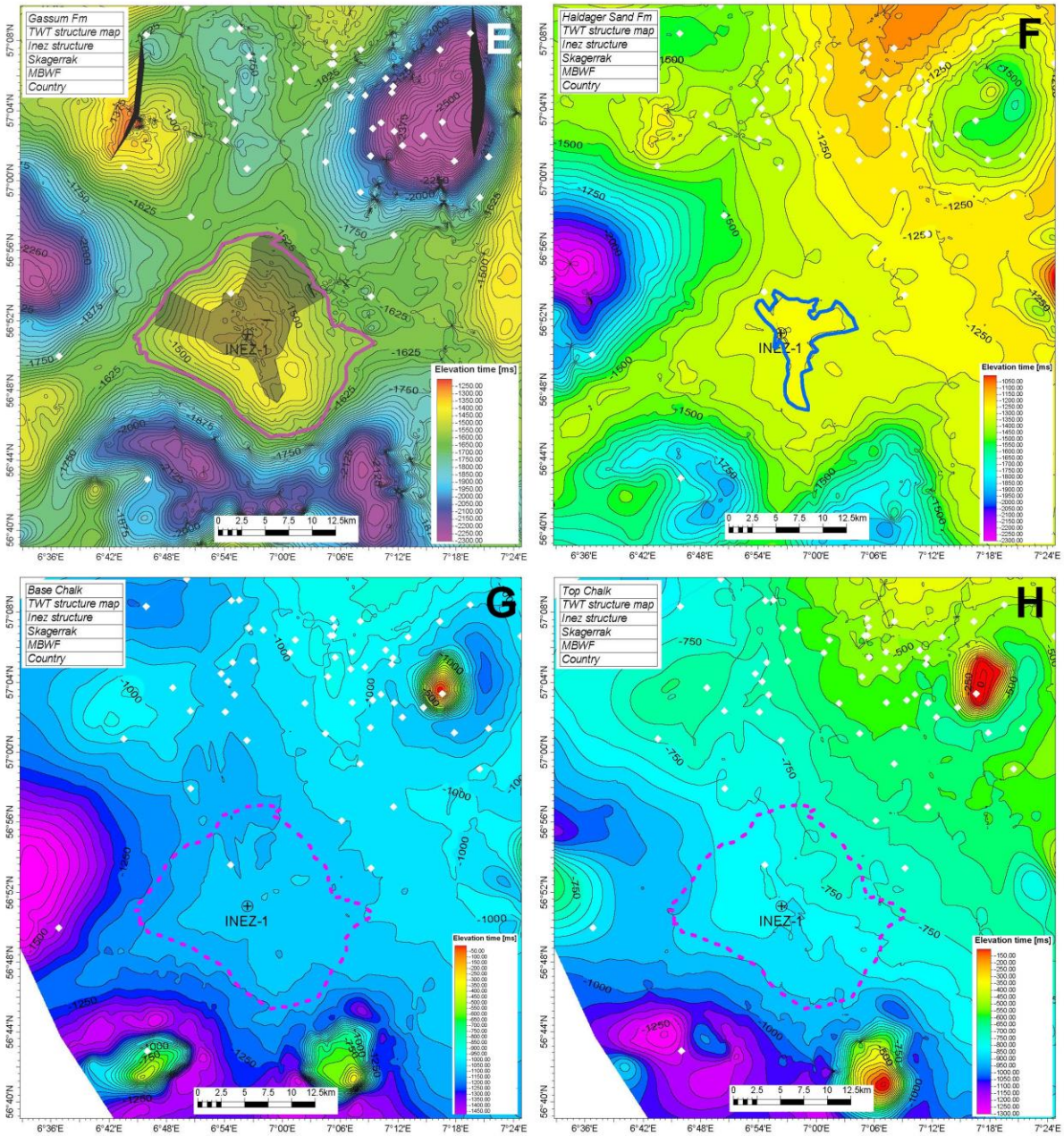

Figure 7.2.1. *Continued.*

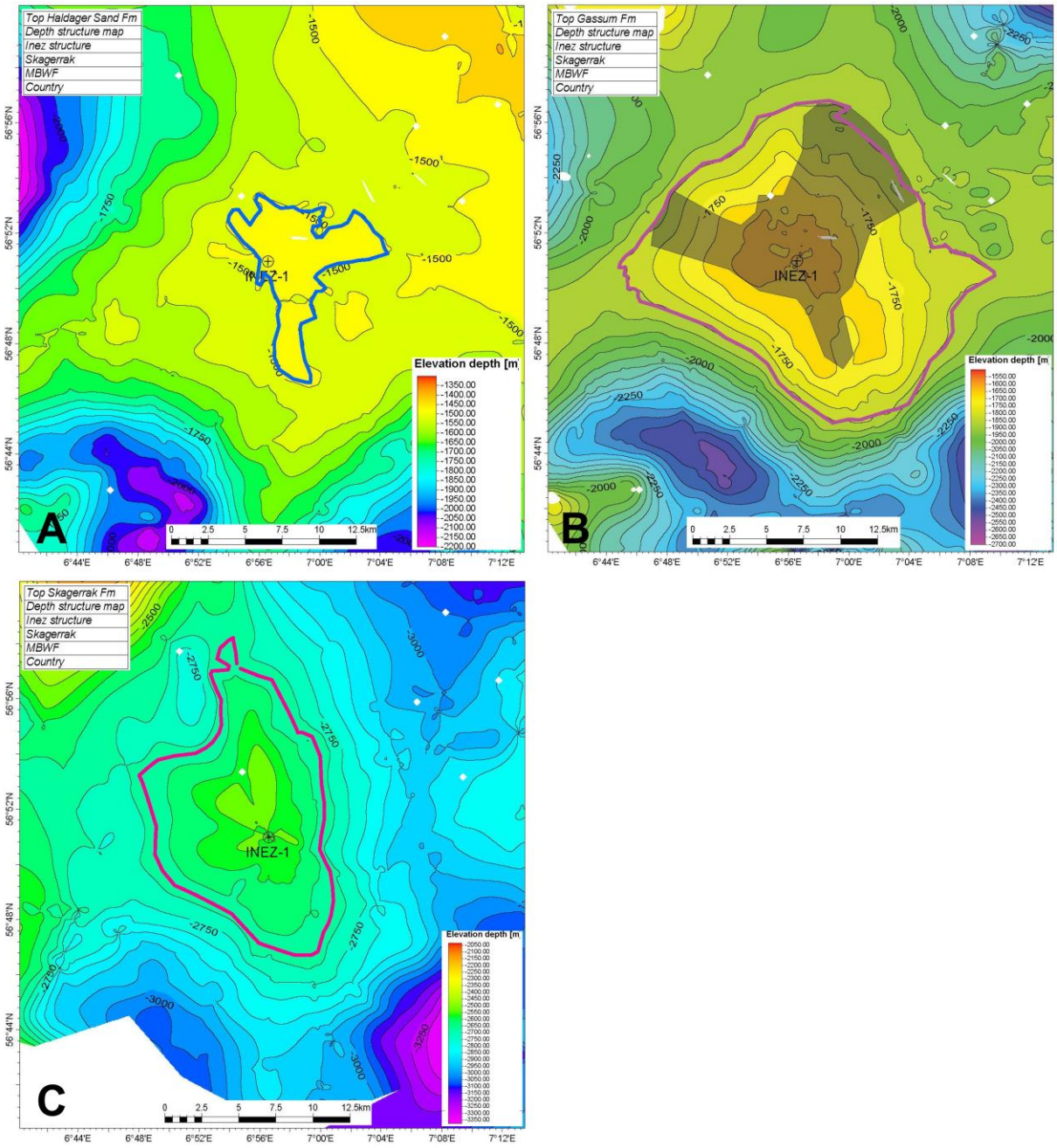

Figure 6.2.2. *Depth structure maps over the top of the three reservoir intervals over the Inez structure.* ***A*** *near-Top Haldager Sand Fm (M Jurassic);* ***B*** *Top Gassum Fm (near top Triassic);* ***C*** *Top Skagerrak Fm (near top M Triassic). Structural closures are outlined with bold signature. Based partly on TGS and Danpec A/S data.*

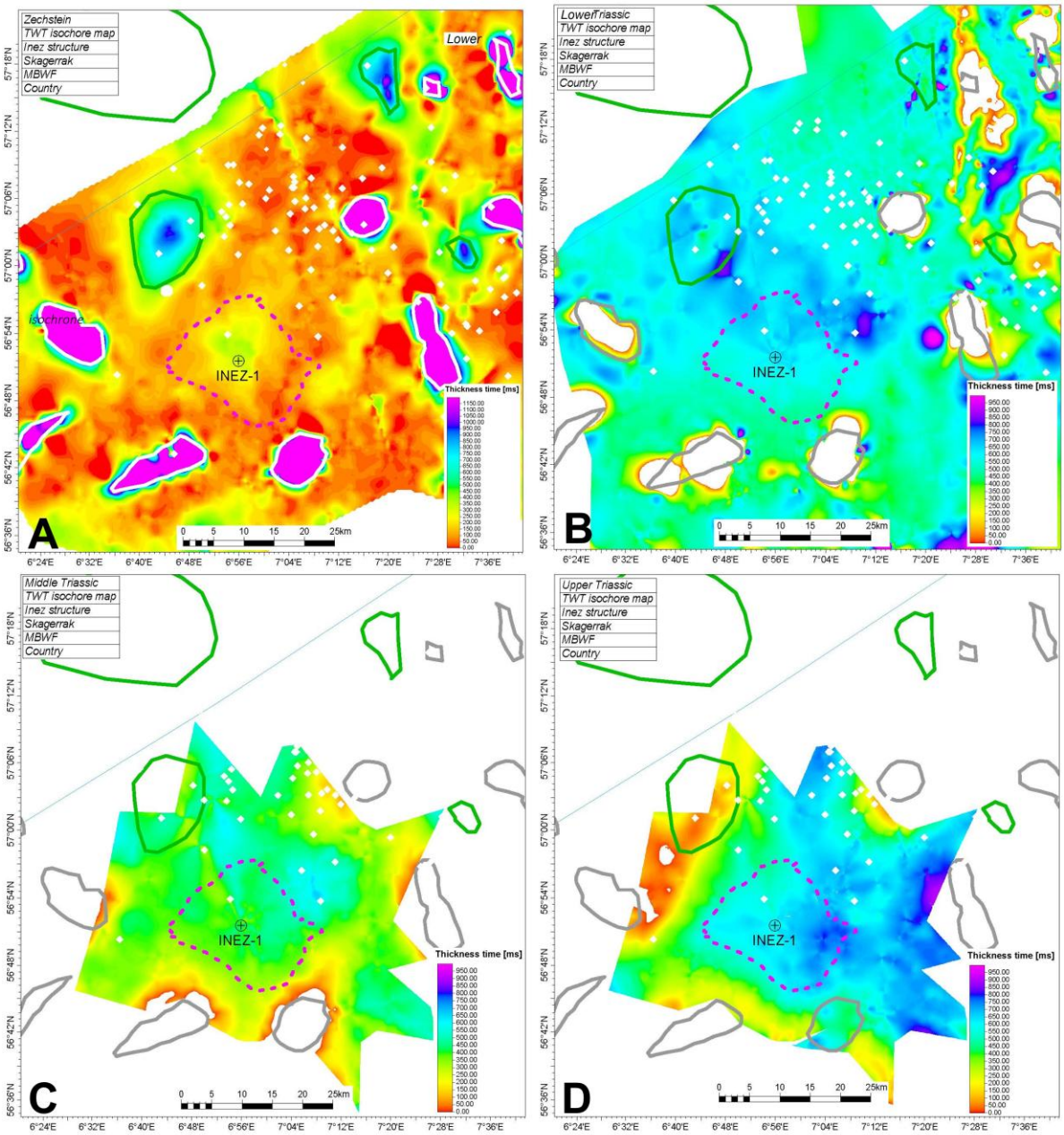

Figure 6.2.3. *TWT isochore maps of the man stratigraphic intervals in the Inez area. Top Gassum Fm closure is indicated with dashed line as georeferenced; salt diapirs/walls and salt pillows are indicated with grey and green polygons, respectively.* ***A*** *Zechstein, note the location of six salt diapirs/salt walls and a large salt pillow surrounding the Inez structure.* ***B*** *~Lower Triassic, thickness variations are subtle relative to other intervals;* ***C*** *~Middle Triassic thickness variations increase with thinning occurring along some salt structure.* ***D*** *~Upper Triassic, considerable thickness variations exist with thinning towards many salt structures and thickening in between reflecting Zechstein salt inflation and withdrawal, respectively. A large salt pillow was rapidly inflating northwest of the Inez structure in the Late Triassic, while pillows continued to grow south and northeast of the Inez area. The first pillow collapse zones around diapirs started to form at this time reflecting local salt piercement.*

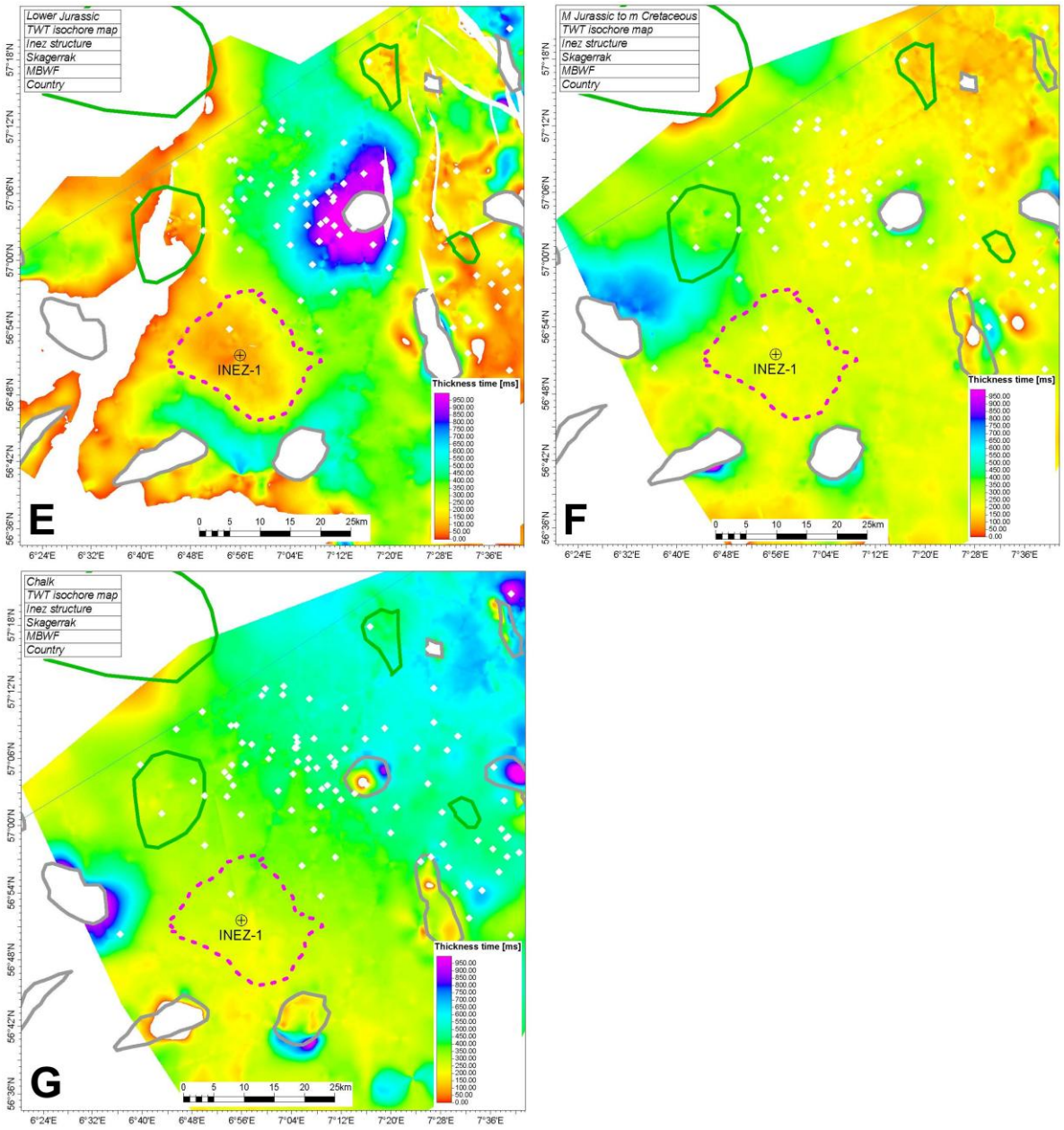

Figure 6.2.3. *Continued.* ***E*** *Lower Jurassic, strong thickness variation also occurs at this level reflecting continued highly active salt kinetics and significant salt piercement at some of the diapirs surrounding the Inez structure resulting in narrow rim synclines (depocenters) along diapirs over collapsing salt pillows. But the variation also reflects the erosional effects of the mid- to Late Jurassic uplift most severe in the west and farthest south, stripping away the Lower Jurassic in part of this area.* ***F*** *mid-Jurassic to mid Cretaceous. Most salt pillows had pierced through the overburden at this stage and diapirs were growing and salt evacuation (and enhanced subsidence) became more focused in narrower zones (pillow collapse zones) surrounding diapirs.* ***G*** *Upper Cretaceous to Paleocene. Thickness variations mainly occur in narrow rim synclines surrounding diapirs. Salt evacuation in the greater Inez area had at this point virtually focused in at narrow pillow-collapse zones around diapirs. Based partly on TGS and Danpec A/S data.*

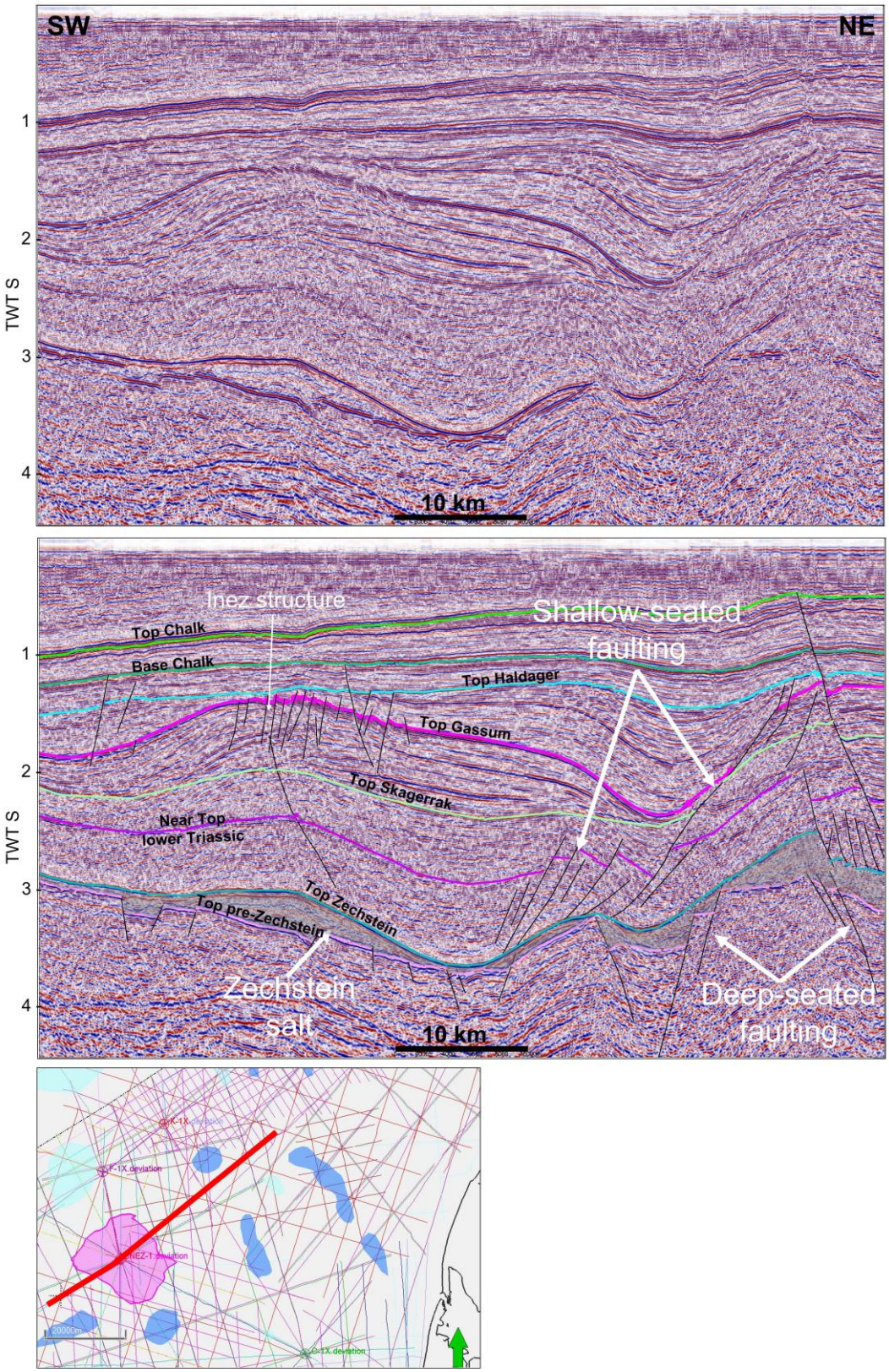

Figure 6.2.4. *Seismic transect across the Inez structure and intersecting the Inez-1 well (uninterpreted and interpreted). The line illustrates the deep-seated faulting underneath the Zechstein evaporites that resulted in a destinct relief at the base Zechstein surface. Most of the faulting likely took place in Middle Troassic through Early Jurassic time, but Zechstein evaporites acted as a decollement decoupling deep-seated faults from shallow-seated Middle Triassic to Early Jurassic faults soleing out in the evaporites. Line location indicated by red line in the lower map Dark and light blue areas are salt diapirs an pillows, respectively. Line RTD81-RE94-42E. Data Courtesy of TGS and Danpec A/S.*

The Inez closure had largely developed by mid-Cretaceous time and subsequent differential salt movement only played a small role in the present closure geometry. Similarly, Late Cretaceous and Cenozoic tilting towards the southwest was less than 1° and did not affect the overall closure geometry much apart from at top-Haldager Sand Fm level, where even a small westward tilt would reduce closure size considerably, thus resulting in the modest present size of the Haldager Sand Fm closure.

In the present-day Danish Skagerrak, only moderate-sized modern earthquakes have been recorded (Sørensen et al. 2011). Sørensen et al. (2011) concluded that earthquakes originate from 11–25 km depth. Accordingly, they must be due to deep seated faulting underneath the Zechstein evaporites. The earthquakes are recorded by an open seismometer grid with stations mostly onshore Denmark, Norway, Sweden and Great Britain, and the calculated locations of earthquake epicentres are with an accuracy of within few to few tens of kilometres. Far the most earthquakes occur within an ellipsoid earthquake swarm (Fig. 6.2.5). The Inez structure is located around 20 km east of the earthquake swarm and only a single modern earthquake has been located within the Inez area but keeping in mind the inaccuracy in locating the earthquakes, this event may also have been located outside the Inez area.

Since recorded modern earthquakes are deep-seated, seismicity associated with slips on shallow seated faults intersecting to near the seabed seems to be seismically quiescent. This may be due to these faults being either inactive or, more likely, that the modern modest displacement occurs as slow creeping. Shallow-seated faults intersecting to near the seabed are focused above salt structures (e.g. Figs. 6.1.1 & 6.1.2). Due to Neogene uplift, and erosional removal of the youngest section apart from a sub-seismic veneer of Pleistocene strata, it is not possible to determine whether faulting has ceased or if it is continuing to the present. Some of the faulting presumably owes to halokinetic motion but some may also be linked with deep-seated motion translated through a Zechstein salt decollement comparable to the Mesozoic faulting. Since major salt structures are located outside the Inez area, such ongoing faulting is less likely to occur here.

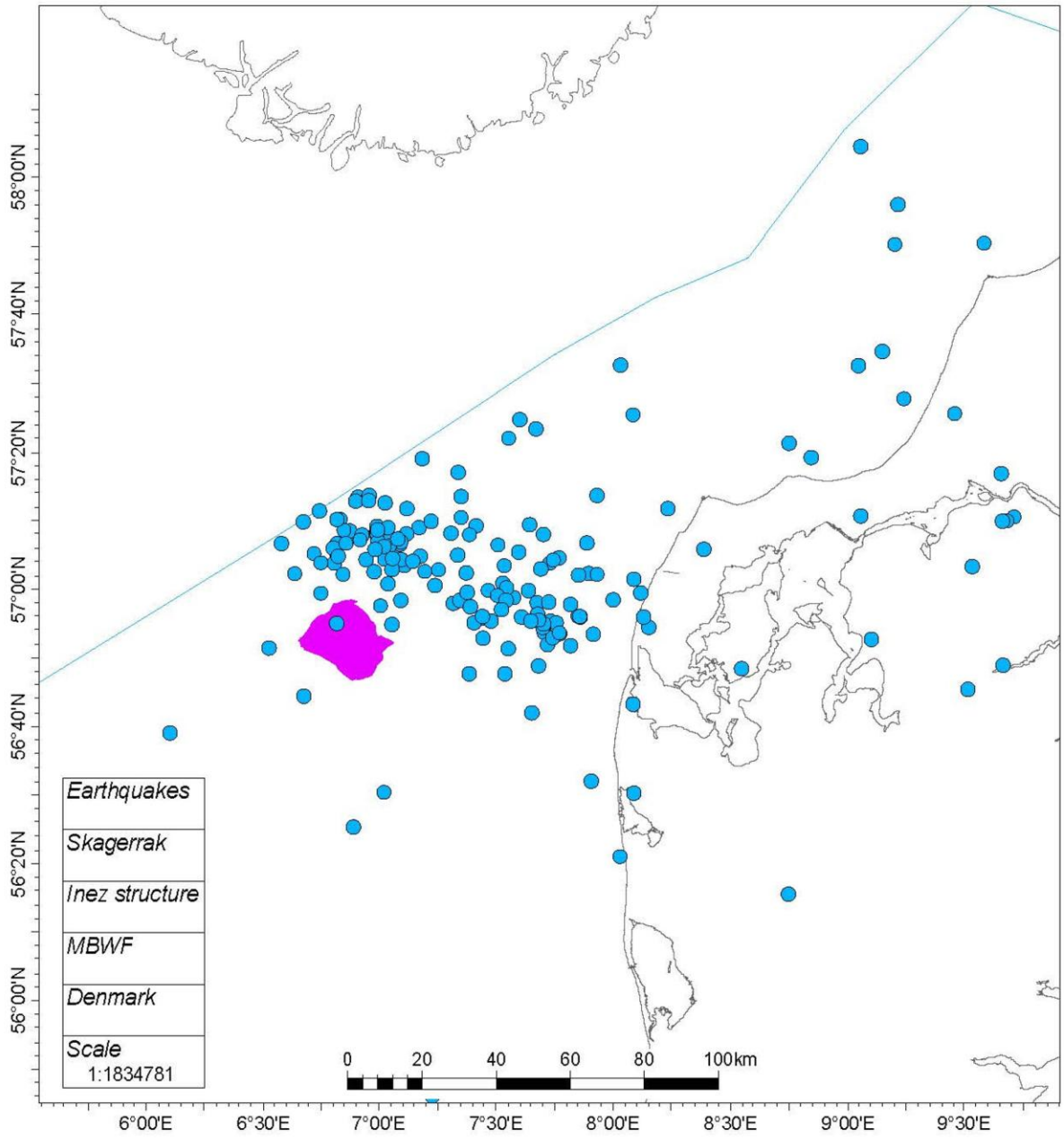

Figure 6.2.5. *Map showing the calculated epicenter of modern earthquakes recorded after 1929 (blue dots). Pink area indicate the location of the Inez structure. Source:*

7. Geology and parameters of the Inez storage complexes

7.1 Reservoirs – Summary of geology and parameters

Inez contains three documented reservoir intervals under structural closure with good to excellent reservoir characteristics: The Gassum Fm, the Skagerrak Fm and the Haldager Sand Fm (Figs. 3.2; 6.1.3; 6.2.2). The surface stratigraphically equivalent to top of the Bunter Sandstone Fm is also characterized by a large Inez-closure (Fig. 6.2.1). However, in the Inez area this surface is considered as an intra-Skagerrak Fm surface. The Gassum Fm has the largest area under closure. It has excellent reservoir characteristics and a gross thickness as defined here around 148 m when including the sandy, reservoir-prone, uppermost Triassic (Rhaetian) interval in the Inez-1 well (Fig. 6.1.3). The Upper Triassic is therefore considered as the primary reservoir. The area under closure for the Haldager Sand Fm is modest (Fig. 6.2.2) and the formation only has a gross thickness of 9 m in the Inez-1 well and a net thickness of only 3 m (Fig. 6.1.3). The formation is therefore treated as a secondary reservoir despite excellent porosity and permeabilities

Based on seismic stratigraphic interpretations correlated with Felicia-1, the Skagerrak Fm is predicted to exist within the deeper part of the Inez structure below the TD of Inez-1 (Fig. 6.1.1). The formation is located at greater depth than the two other reservoir units but has a considerable area under closure and may have a very large gross-thickness (Fig. 6.2.3). Reservoir characteristics are uncertain, and the Skagerrak Fm is for now treated as a secondary reservoir.

7.1.1 The primary reservoir: The Gassum Formation

Inez-1 intersects the Inez structure next to the apex of the Gassum Fm closure. Nielsen and Japsen (1991) picked the top of the Gassum Fm in the Inez-1 well at 1633 m – 26 m above where we do. They picked it at the top of the Hettangian at the top of a 2 m thick sandstone interbed encased in an entirely shaly succession. We here attribute this sandstone bed and the Hettangian shaly succession to the Fjerritslev Fm. Instead, we pick the top of the Gassum Fm in 1659 m depth (1695 m measured depth) at the top of the thick sand-dominated unit of Rhaetian age. We pick the base of the Gassum Fm in Inez-1 at 1807 m bmsl (1843 m measured depth) at the base of the sand-dominated interval that rests on a mudstone-dominated succession containing traces of anhydrite continuing to the base of the well. The Gassum Fm sandstones intercalate with mud- and limestone interludes. The Gassum Fm as defined here has a net to gross (N/G) ratio of around 0.59, a gross thickness of 148 m with a net reservoir thickness of 86.7 m, an average log derived porosity of 20.3% and a corresponding log derived permeability of 442 mD (Table 7.1.1.1). The underlying lower Rhaetian Oddesund/Vinding Fm also includes a few reservoir beds with an average PHIE of 0.16, but these are excluded from the primary reservoir of the Gassum Fm. The erratic pattern of the Vshale-curve through the Rhaetian is suggested to reflect a floodplane, marginal marine and near-shore depositional environment, further supported by the paleontological analyses (King et al. 1978).

Table 7.1.1.1 *Reservoir properties derived from the Inez-1 well*

Reservoir properties for Inez-1											
	Well	**Zones**	**Flag Name**	**Top**	**unit**	**Gross (m)**	**Net (m)**	**Net to Gross**	**Av_VSH**	**Av_PHIE**	**Est_PERM (mD)**
1	Inez-1	Haldager Sst	RES	1559	M	9.14	2.95	0.32	0.265	0.255	871
2	Iinez-1	Gassum Fm	RES	1695	M	147.7	86.7	0.59	0.265	20.3%	442

Gassum Fm sandstones in Inez-1 is typically friable, fine-grained, angular to sub-rounded, well-sorted and occasionally felspathic (Chevron 1978). Olivarius et al. (2019) pointed out that the feldspar content has occasionally been underestimated in original well-site studies in the Danish western part of the Norwegian–Danish Basin and that Gassum Fm sandstones are often arkosic in nature. An arkosic and occasionally micaceous composition of part of the Gassum Fm sandstones, implies a higher concentration of radioactive elements compared to clean quarts sandstones. This increases the uncertainty of the petrophysical lithological interpretations, possibly leading to an underestimation of the sandstone content, and thus, an underestimation of the reservoir potential of the formation.

Seismic data document a southward depocenter migration during the latest Triassic – earliest Jurassic across the Inez area in response to southward salt motion. The upper part of the Gassum Fm, having the best reservoir properties in Inez-1, is therefore thickest developed over the southern part of the Inez structure (Fig. 6.1.4). The distinct seismic facies change observed within the same interval interpreted to reflect increasingly marine deposits toward the south documents a further lateral variation in lithology and deposition across the Inez structure. Olivarius et al. (2019) interpreted a provenance rooted in present day southern Norway for the Hettangian-Rhaetian sandstones in Felicia- and J-1. This is compatible with this suggested north–south variation in deposition and the general interpretation of the proximal parts of the basin being located to the north and east with the distal basin toward the south (Michelsen et al. 2003).

7.1.2 Secondary reservoir 1: Skagerrak Formation

The Skagerrak Fm is of Early to earliest Late Triassic age. It grades laterally from alluvial fan deposits formed along the fringe of the Scandinavian craton to braided river deposits formed more distally in the Norwegian–Danish Basin (Olsen 1988). The Skagerrak Fm has a high, although variable, sandstone content. In the central Norwegian–Danish Basin, the formation describes an overall retrogadational trend. The retrogradation is reflected in a graduation from proximal braidplain sediments in the Lower Triassic over intermediate braidplain deposits in the Middle Triassic to distal braidplain accumulations in the lowermost Upper Triassic. The retrogradation resulted in an upward decrease in the sand-/mudstone-ratio (Bertelsen 1980; Olsen 1988).

The Skagerrak Fm is thickly developed in the basin and exceeds 2 km in thickness in the Felicia-1 well. A comparable thickness is estimated within the Inez structure based on seismic correlation. The formation consists of interbedded, arkosic sandstones, siltstones and claystones together with variable amounts of anhydrite (Statoil 1988). Sandstones are fine- to coarse-grained, typically poorly sorted with angular–subangular grains (Bertelsen 1980). Potential in-

ternal barriers or seals are rare (Petersen et al. 2008). At the crest of the Inez structure, the top of the Skagerrak Fm is picked around 2500 m depth (Fig. 6.2.2). Considering a Neogene net denudation of around 300 m of the Inez area (Petersen et al. 2008), the top of the Skagerrak Fm has been buried to a maximum depth of around 2.8 km. This is slightly less than, the estimated maximum burial depth of the top of the Skagerrak Fm of around 3.2–3.5 km in the Felicia well (Japsen et al. 2007). In the Felicia-1 well, only the uppermost 117 m of the Skagerrak Fm has a reservoir potential. The underlying part of the Skagerrak Fm has lost its reservoir potential due to burial diagenesis. The reservoir-prone Skagerrak Fm in the Inez structure may thus be thicker than in the Felicia-1 well due to the lower maximum burial depth. In the Felicia-1 well the upper 117 m of the formation has a N/G of 0.38 and an average porosity of roughly 0.15. The reservoir potential decreases downwards through the formation mainly due to burial depth, and the lower half of the formation is virtually devoid of reservoir potential in that well. Based on the measured relationship between porosity, permeability and maximum burial depth of the Skagerrak Formation in Danish onshore Skagerrak Fm-cores, average porosities and permeabilities around 0.22 and 260 mD in clean sandstones is expected in the uppermost Skagerrak Fm in the Inez structure. The sandstone composition likely varies however, and the actual total reservoir average porosity may be lower. On the other hand, N/G may be higher than 0.38 since this number reflects only the parts of the upper Skagerrak Fm preserving porosities of at least 0.12 in the Felicia-1 well that has been roughly 400–700 m deeper buried than at the Inez structure. For simplicity in the storage capacity modeling, a porosity range similar to those measured from the Gassum Fm has been used, while a N/G of 0.38 has been used as the most likely case similar to that measured in the uppermost 117 m of the Skagerrak Fm in Felicia-1. Since Skagerrak Fm at the Inez structure has not been as deeply buried as in the Felicia-1 well, the reservoir thickness most likely exceeds the 117 m measured at Felicia-1, and for modelling purposes, the most likely case has been set to 175 m filling out the closure relief at Skagerrak Fm level.

7.1.3 Secondary reservoir 2: Haldager Sand Formation

The Haldager Sand Fm is around nine meters thick in the Inez-1 well where it was met in 1522 m depth bmsl (1559 m measured depth. Lithologic and reservoir information apart from a single sidewall core derives entirely from electrical logs. The formation consists primarily of well-sorted, sub-angular, coarse-grained, and loosely consolidated porous sandstones with an average porosity of around 26%, a derived average permeability of more than 871 mD and an estimated N/G of around 0.32. The formation rests on the mid-Cimmerian unconformity and is interpreted to having formed as a transgressive sand following the Middle Jurassic uplift in a fluvio-marine environment.

7.2 Seals – Summary of geology and parameters

Three reservoir/seal pairs are identified over the Inez structure. These are the Gassum/Fjerritslev fms (primary), the Skagerrak/Oddesund fms (secondary) and the Haldager Sand/Børglum fms (and overlying Upper Jurassic–Lower Cretaceous fine-grained units) [secondary]. The seals are described in the following sections.

7.2.1 The primary seal (for the Gassum Fm): The Fjerritslev Fm

The Lower Jurassic Fjerritslev Fm works as seal for the Gassum Fm reservoir. The formation consists of a marine, uniform, shaly, slightly calcareous succession with thin silty/sandy interbeds. Fjerritslev Fm is subdivided into four members F-I to F-IV, from base to top, respectively. Over the crest of the Inez structure, in Inez-1, the 127 m thick Fjerritslev Fm consists entirely of the F-I member. The seal is met in 1532 m depth bmsl in Inez-1 but has been buried probably a

few hundred meters deeper prior to Neogene uplift and erosion (Petersen et al. 2003). Over some of the Inez structure, faults propagate upwards from the Gassum Fm and into the Fjerritslev Fm and the lower part of the latter formation is probably somewhat faulted with fault offsets typically in the range of a few tens of meters or less but dying out upwards through the formation (Fig. 6.2.4). These faults therefore appear to have formed in the (Late Triassic and) Jurassic and to have been inactive ever since.

Part of the Fjerritslev Fm is rich in organic matter. TOC (Total Organic Carbon) varies and is typically richest in the upper F-III and F-IV members (Petersen et al. 2008). The sealing properties are not expected to have been impacted by the organic content since the Fjerritslev Fm at Inez is thermally immature and organic matter have not been transformed into hydrocarbons migrating out of the formation creating fluid migration pathways. Furthermore, Guiltinan et al. (2017) demonstrated that even thermally mature carbonaceous shales with TOC of up to 8% may have sealing potential. On a regional average, F-I has a TOC of 0.97% with maximum values of around 5 %. In the Inez-1 well, a slightly higher average TOC of 1.07% has been measured but still well within the range for good seals.

The Fjerritslev Fm thickens over the northern, eastern and southern flanks of the Inez structure partly because of increased Early Jurassic subsidence and deposition in the rim-synclines flanking Inez but also partly due to deeper Middle to Late Jurassic erosion along the mid-Cimmerian unconformity over the crest of the structure and to the west. While Fjerritslev members II to IV lacks here, some of them may therefore occur over the are therefore expected over the northern, eastern and southern flanks.

Clay minerals in the Fjerritslev Fm mudstones primarily consist of kaolinite and illite but also contains some smectite (Mathiesen et al. 2022). Quarts comprise up to half of the bulk mineral composition above the clay-size fraction. A high clay content reduces the size of pore throats, permeability, and thus increase the capillary entry pressure (*Katsube og Williamson, 1994*). Experiments simulating reservoir conditions on Fjerritslev Fm samples from the onshore Stenlille-2 well demonstrated a fluid permeability of 3 nD making it an excellent cap rock (Springer et al. 2010). Springer et al. (2010) further demonstrated a capillary entry pressure of 70 bar for a massive Fjerritslev Fm mudstone layer during a super-critical (sc) CO_2 seal capacity test. This corresponds to a capability of retaining an at least 1000 m high vertical column of $scCO_2$ - much thicker than the Gassum reservoir at the Inez structure.

Mudlog gas data measured at Stenlille-19 and Voldum-1 wells onshore demonstrates an abrupt fall in light natural gas from the underlying Gassum Fm reservoir to the overlying F-I member of the Fjerritslev Fm, thus confirming the tight sealing of the unit (Andersen et al. 2022). The background gas content in the Inez-1 well is modest. It consists entirely of C1 and is constant from the Gassum Fm reservoir and into the overlying Fjerritslev Fm seal. The gas does therefore not offer information about the effectiveness of the Fjerritslev Fm seal since the gas most likely represent small amounts of *in situ* biogenic gas.

With the high sealing capacity of the Fjerritslev Fm in general and the 127 m thickness at Inez in specific, the seal risk *sensu* Bruno et al (2014) is low. However, the overall Fjerritslev Fm seal characterisation is based on a restricted number of analyses most of which were not performed on material from Inez-1 or neighbouring North Sea wells and therefore needs to be substantiated by further analysis. The faulting in part of the Fjerritslev Fm over some of the Inez structure and its potential effect on sealing integrity requires further attention.

The Fjerritslev Fm is by Nielsen and Japsen (1991) considered to be thinly overlain by the Haldager Sand Fm. Following their concept, the sandstone unit only describes a small structural closure. The closure is lager if the sandy unit instead belongs to the Fjerritslev Fm as discussed above. The fine-grained Upper Jurassic Børglum Fm together with the Frederikshavn Fm and Lower Cretaceous units above the Haldager Sand Fm have a combined thickness of 274 m and is treated below.

7.2.2 Seals of the secondary reservoir/seal pairs: Oddesund Fm sealing the Skagerrak Fm

The Oddesund Fm of Carnian to early Rhaetian/Norian age is anticipated to cap the Skagerrak Fm in the Inez structure but has not been penetrated by the Inez-1 well. The Oddesund Fm generally consists of variegated red-brown, brown and grey, anhydritic and calcareous clay- and siltstones with thin, sporadic dolomitic limestone, sandstone and marl interbeds. The formation formed in a hot and dry to semi-dry environment (Bertelsen 1980). In depocenters, halite occurs and laterally grades into anhydrite as a fringing facies that in turn grades into continental clastic red beds along the margins farther away. The Oddesund Fm formed in episodically flooded sabkhas, playas/ephemeral lakes. Fluvial deposition probably occurred episodically along the basin margin during the most humid periods, while halite deposition took place during dry periods in permanently waterlogged hyper-saline lakes/lagoons restricted to depocenters. These hyper-saline water bodies possibly connected to the Tethys through a narrow corridor at the south-eastern end of the basin (Bertelsen 1980). In the Felicia-1 well situated next to the Triassic depocenter in the Fjerritslev Trough, the Oddesund Formation is dominated by claystones, often with a high content of anhydrite, and subordinate silty, sandy and halite intervals. Compared with the Felicia area located at the margin of the Fjerritslev Trough, the Inez area is situated closer to the basin margin at the northern edge of the Ringkøbing–Fyn High. Only the uppermost part of the Oddesund Fm may have been reached in the Inez-1 well, but the gross-depositional setting proposed by Bertelsen (1980) may favour a lithology dominated by fine-grained red beds with anhydrite and dolomite interbeds. While the Inez structure is located in a local Late Triassic depocenter, there are no signs of differential salt motion within the Oddesund Fm-interval and halite may be rare or even absent. Overall, the Oddesund Fm are likely to have good seal capacity over the Skagerrak Fm in the Inez area. Fjerritslev Fm forms a secondary seal with respect to the Skagerrak Fm/Oddesund Fm reservoir seal pair.

7.2.3 Seals of the secondary reservoir/seal pairs: The Upper Jurassic to Lower Cretaceous sealing the Haldager Sand Fm

In Inez-1, the Upper Jurassic to Lower Cretaceous consists of the Børglum, Frederikshavn and Vedsted formations having a total thickness of roughly 273 m. The existing seismic coverage over the Haldager Sand Fm closure at the Inez structure does not reveal faulting of the Upper Jurassic to Lower Cretaceous interval. The Børglum Fm of Late Jurassic age comprises a 46 m thick claystone succession that rests directly on the Haldager Sand Fm forming a uniform, fine-grained succession (Fig. 6.1.3) dominated by thermally immature, homogenous, often calcic shales with a relatively high TOC (averaging 1,68 in the J-1 well). The formation formed in an open marine environment and has a low content of siltstones and minor sandstones (Michelsen et al. 2003).

Mudgas concentration is low and consists entirely of C1. There is no change in gas concentration from the Haldager Sand Fm reservoir and into the overlying Børglum Fm seal and the gas does not offer information about the effectiveness of the Børglum seal since the gas most likely derive from small amounts of *in situ* biogenic gas.

Børglum Fm is overlain by 83 m Frederikshavn Fm (Fig. 6.1.3). The Frederikshavn Fm consists mainly of claystones but includes a 12 m thick siltstone-dominated interval with a few sandy intercalations located in the upper part.

The overlying 144 m thick Vedsted Fm is clay- to mudstone dominated but contains few meter-thick silt and sand interbeds. Springer et al. (2010) showed that the formation (anticipated as the Børglum Fm) has good sealing potential based on analyses made under reservoir conditions of core material from a Stenlille bore hole.

The thickness of the Børglum Fm and the overlying fine grained succession far exceeds the 30 m seal thickness considered as the minimum thickness for having a small seal risk (Bruno et al. 2014). The Chalk Group generally has high porosities but low permeabilities. In Central Graben, the fair reservoir characteristics is primarily restricted to the upper part of the chalk, while the lower part more resembles a seal. Some of the 417 m thick chalk package and most of the overlying roughly 150 m thick Paleogene mudstones over the Inez structure are likely to have good sealing characteristics. However, no closure exists at the base of this level and neither the chalk nor the Paleogene is treated as secondary seals *sensu stricto*.

8. Discussion of storage and potential risks

8.1 Volumetric input parameters

8.1.1 Gross rock volume

The Gross Rock Volumes of the three Inez structure reservoir units have been calculated using the Area and Thickness vs. Depth methodology described by e.g. James et al. (2013). Area vs depth tables have been extracted for the mapped and depth converted top reservoir surfaces and reservoir gross thicknesses were estimated from petrophysical work on the local well. A most likely volume-scenario was establish based on model values derived directly from the mapping and petrophysical analysis. In order to capture the uncertainty on the GRV across the Inez structure, a minimum and maximum scenario was also calculated. As shown in Figure 8.1.1.1.1, three scenarios were set up for the areal extent to cover uncertainty in interpretations, mapping and depth conversion and scenarios were also built for the gross thickness and spill point.

GRV from area and thickness vs depth calculations were constructed for the three scenarios defined by min., mode (most likely) and max. as exemplified in Figure 8.1.1.1. It is assumed that the GRV distribution follows a Pert distribution defined by the min., mode and max. values. The Pert distribution is believed to give suitable representation for naturally occurring events following the subjective input estimates (Clark 1962). For the Gassum, Haldager Sand and Skagerrak fms reservoir units the assumption input for the GRV and the GRV scenarios are given in Table 8.1.1.1.

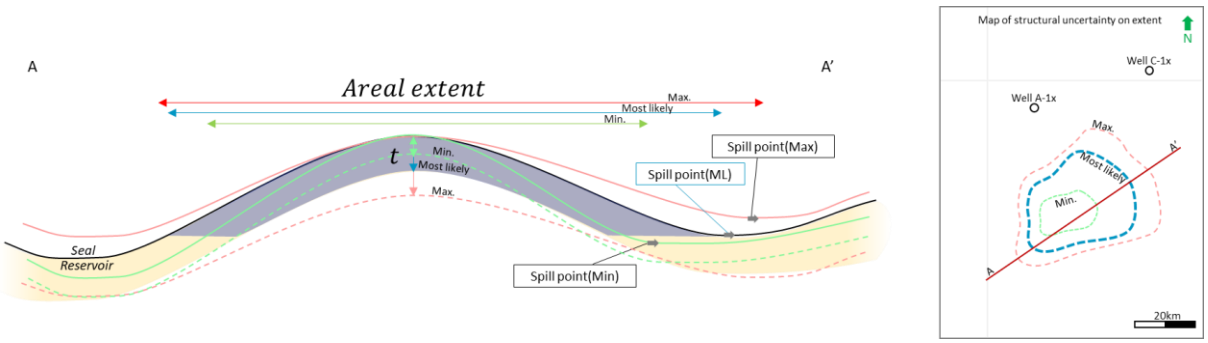

Figure 8.1.1.1. *Conceptual profile (A-A') across a potential structure. The uncertainty in mapping the structure results in the hypothetically min. and max. scenarios looking very different from the most likely mapped scenario. Variance in area and in thickness (t) average assumptions will affect the gross rock volume of the structure.*

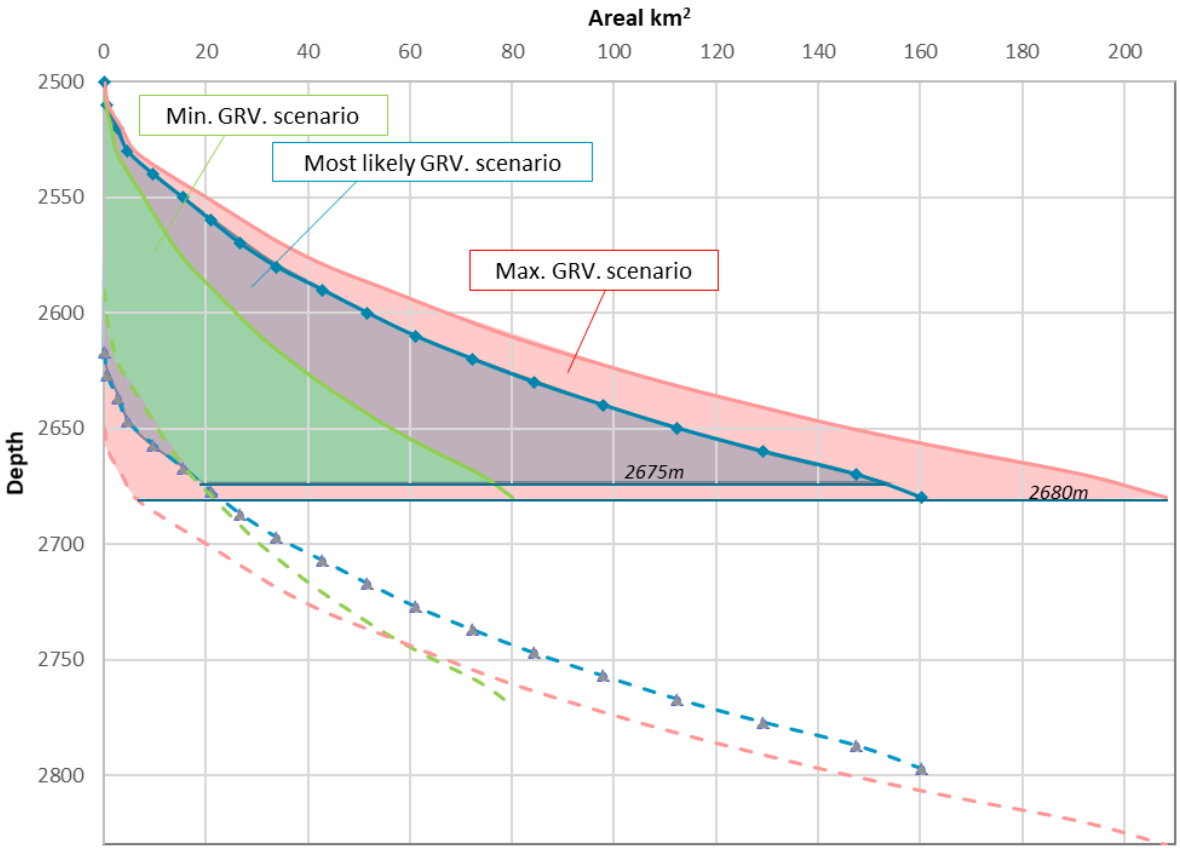

Figure 8.1.1.2. *Area and Thickness vs. Depth plots of the Inez structure. GRV is calculated from a Top surface and average thickness assumption with 10 meters depth increments for both the min., max. and the most Likely (mode) scenarios. The max./min. GRV ratio is c. 5 in this example.*

Table 8.1.1.1. *Gross Rock Volume assumption input and resultant GRVs*

Unit	Apex [m,TVDSS]	Spill point [m, TVDSS]			Area [km²]			Thickness [Gross, m]			GRV [1e⁶m³]		
		Min.	Mode	Max.	Min.	Mode	Max.	Min.	Mode	Max.	Min.	Mode	Max.
INEZ Haldager	1461	1500	**1500**	1510	30,6	**61,1**	105,0	5	**9,14**	20	114,1	**417,0**	1.676,0
INEZ Gassum	1592	1850	**1850**	1875	150,5	**301,0**	452,4	100	**147,7**	200	11.059,0	**28.076,7**	49.666,2
INEZ Skagerrak	2501	2675	**2675**	2677	76,9	**153,9**	208,1	90	**175**	250	3.710,5	**8.780,0**	12.914,9

8.1.2 Net to Gross ratio

The N/G-ratios estimated from the petrophysical analysis of the Inez-1 well is considered reasonable average N/G-values across the entire structure and is defined as the mode of the distribution. Some variance is expected due to lateral variation. To reflect this uncertainty, a distribution for the average N/G was constructed by defining the min. and max. of the distribution as +/- 20% (minor adjustments may occur). A Pert distribution has been applied.

8.1.3 Porosity

The porosity (ϕ) was estimated from petrophysical analysis of the Inez-1 well as described in Chapter 7.1. The well-derived estimate is considered as a reasonable average porosity across the entire structure (set as Mode). Some variance is expected as lateral and depth variations may occur. To reflect this, an average porosity distribution has been constructed defining the min. and max. of the distribution as +/-20% (minor adjustments may occur). A Pert distribution for this element has been applied.

8.1.4 CO_2 density

The average in-situ density of CO_2 was estimated using the 'Calculation of thermodynamic state variables of carbon dioxide' web-tool essentially based on Span and Wagner (1996) [http://www.peacesoftware.de/einigewerte/co2_e.html]. The average reservoir pressure was calculated on the assumption that the reservoir is under hydrostatic pressure and a single pressure point midway between apex and max spill point was selected representing the entire reservoir. Temperature for this midway point was calculated assuming a seabed temperature of 4°C and a geothermal gradient derived from the Inez-1 well. Assumptions and calculated densities for the individual reservoir units are tabulated in Table 8.1.4.1. For a quick estimation of the uncertainty on CO_2 density, various P-T scenarios were tested and in general terms a -5% (min.) and +10% (max.) variation from the calculated mode was applied for building a distribution (Pert). All calculations showed that CO_2 would be in supercritical state.

Table 8.1.4.1. *CO_2 fluid parameter assumption and estimated values*

Unit	Apex depth [TVDSS, m]	Spill point depth [TVDSS, m]	Structural relief [m]	Water depth [m]	Pressure HydroS.[MPa]	GeoThermal grad. [C/km]	Mid Res. Temp. [C]	CO2 density [Kg / m3]
Inez_Haldager_S_Fm	1462	1510	48	35,05	14,58	34	53,3	641,7
Inez_Gassum_Fm	1592	1875	283	35,05	17,01	34	61,7	644,0
Inez_Skagerak_ Fm	2500	2675	175	35,05	25,38	34	90,8	639,2

8.1.5 Storage efficiency

Storage efficiency is heavily influenced by local subsurface confinement, reservoir performance, compartmentalisation etc. (geological factors) on the one hand, and injection design and operation (financial controlled factors) on the other (Wang et al. 2013). A sufficient analogue storage efficiency database is not available to this study and accurate storage efficiency factor-ranges lacks at this early stage of maturation. This emphasises the need for further investigations of subsurface and development scenarios to better understand the potential storage efficiency ranges. In this evaluation, a range from 5% to 15% with a mode of 10% is used as a possible range, although we emphasise the need for further work on this. A Pert distribution for this element has also been applied.

In Tables 8.1.5.1 through 8.1.5.3, input parameter distributions are listed (all selected to follow Pert distributions defined by min., max. and mode). An example of parameter distributions is displayed in Figure 8.1.5.1..

Table 8.1.5.1. *Input parameters for the Haldager Sand Fm within the Inez structure*

Parameter	Assumption		
	Min	Mode	Max
GRV ($10^6 m^3$)	114	417	1676
Net/Gross	0,2	0,317	0,5
Porosity	0,2	0,255	0,3
Storage eff.	0,05	0,1	0,15
In situ CO_2 density (kg/m^3)	609,6	641,7	705,9

Table 8.1.5.2. *Input parameters for the Gassum Fm within the Inez structure*

Parameter	Assumption		
	Min	Mode	Max
GRV ($10^6 m^3$)	11059	28076	49666
Net/Gross	0,4696	0,587	0,7044
Porosity	0,1624	0,203	0,2436
Storage eff.	0,05	0,07	0,15
In situ CO_2 density (kg/m^3)	611,8	644	708,4

Table 8.1.5.3. *Input parameters for the Skagerrak Fm within the Inez structure*

Parameter	Assumption		
	Min	Mode	Max
GRV ($10^6 m^3$)	3710,5	8781	12915
Net/Gross	0,3056	0,382	0,4584
Porosity	0,1624	0,203	0,2436
Storage eff.	0,05	0,1	0,15
In situ CO_2 density (kg/m^3)	607,2	639,2	703,1

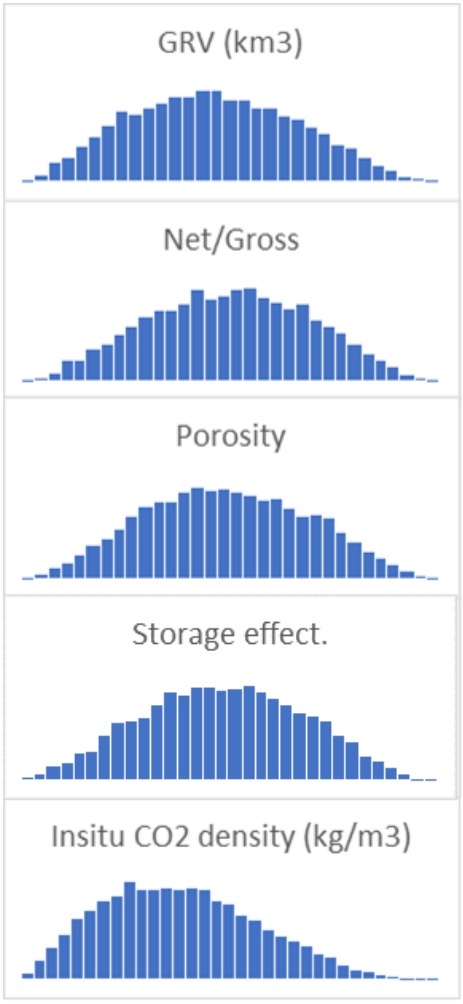

Figure 8.1.5.1. *Example of the distribution shapes (Pert dist.) for the input paremeters (Table 8.1.5.2.).*

8.2 Storage capacity Results

The modelled volumetrics was made on the assumption of the presence of an efficient reservoir/seal pair capable of retaining CO_2 in the reservoir, which needs to be tested by further geological investigation. In Tables 8.2.1 through 8.2.3, the results of the Monte Carlo simulations are tabulated. The tables indicate both the pore volume available within the trap (full potential above structural spill), the effective volume accessible for CO_2 storage (applying the Storage Efficiency factor to pore volume) and mass of CO_2 in mega-tons (MT) that can be stored. The tables present the 90%, 50% and 10% percentiles (P10, P50 and P10) corresponding to the chance for a given storage volume scenario to exceed the given capacity/volume value. Mean values of the resultant outcome distribution are also tabulated and is considered the "best" single value representation for the entire distribution. A mean storage capacity of 3.1 MT CO_2 is calculated for the Haldager Sand Fm and 43.2 MT CO_2 for the Skagerrak Fm, while a much larger mean storage capacity of 177.6 MT CO_2 is modelled for the Gassum Fm confirming it as the primary reservoir for the Inez structure. A combined unrisked storage potential of 224,8 MT CO_2 is calculated for all three reservoir units with a range between 148.6 MT CO_2 (P90) and 310.2 MT CO_2 (P10) and a P50 of 216.2 MT CO_2 (Table 8.2.4 & Figure 8.2.1.). Due to the variability-ranges of the behind-lying factors, the modelled storage capacity has a significant range and is associated with uncertain. As illustrated in Figure 8.2.2, the largest storage capacity uncertainty is linked with the uncertainty in reservoir gross rock volume and storage efficiency. In comparison, CO_2 density at reservoir conditions, is of minor concern.

Table 8.2.1. *Inez structure Haldager Fm storage capacity potential*

Results	P90	P50	P10	Mean
Buoyant trapping pore volume (Km^3)	0,020	0,044	0,082	**0,048**
Buoyant eff. storage volume (Km^3)	0,002	0,004	0,008	**0,005**
Buoyant storage capacity (MT CO_2)	1,2	2,8	5,5	**3,1**

Table 8.2.2. *Inez Structure Gassum Fm storage capacity potential*

Results	P90	P50	P10	Mean
Buoyant trapping pore volume (Km^3)	2,207	3,364	4,724	**3,422**
Buoyant eff. storage volume (Km^3)	0,161	0,259	0,406	**0,273**
Buoyant storage capacity (MT CO_2)	103,8	168,1	263,7	**177,6**

Table 8.2.3. *Inez structure Skagerrak Fm storage capacity potential*

Results	P90	P50	P10	Mean
Buoyant trapping pore volume (Km^3)	0,469	0,666	0,870	**0,669**
Buoyant eff. storage volume (Km^3)	0,043	0,065	0,094	**0,067**
Buoyant storage capacity (MT CO_2)	27,4	42,1	60,7	**43,2**

Table 8.2.4. *Inez structure combined storage capacity potential*

Results	P90	P50	P10	Mean
Buoyant storage capacity (MT CO_2)	148,6	216,2	310,2	**224,8**

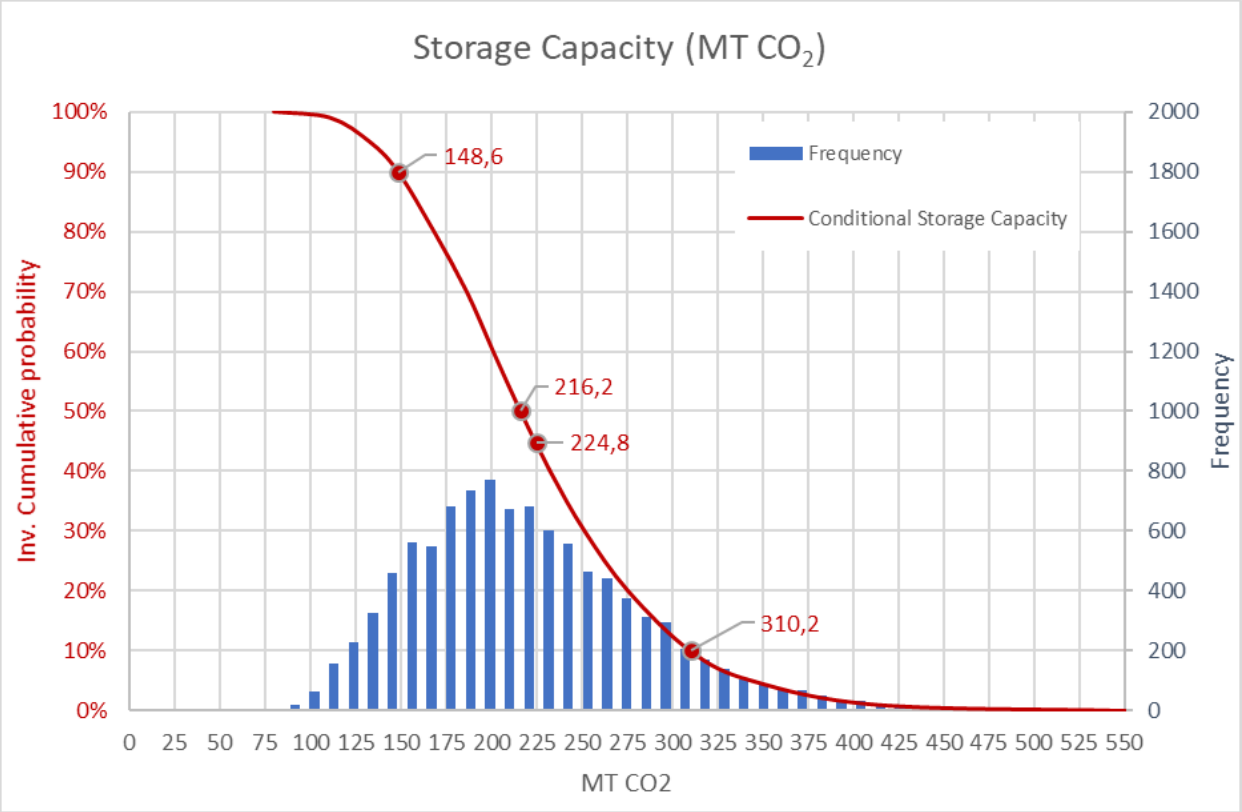

Figure 8.2.1. Modelled statistical distribution of the *combined storage capacity potential in the Inez structure.*

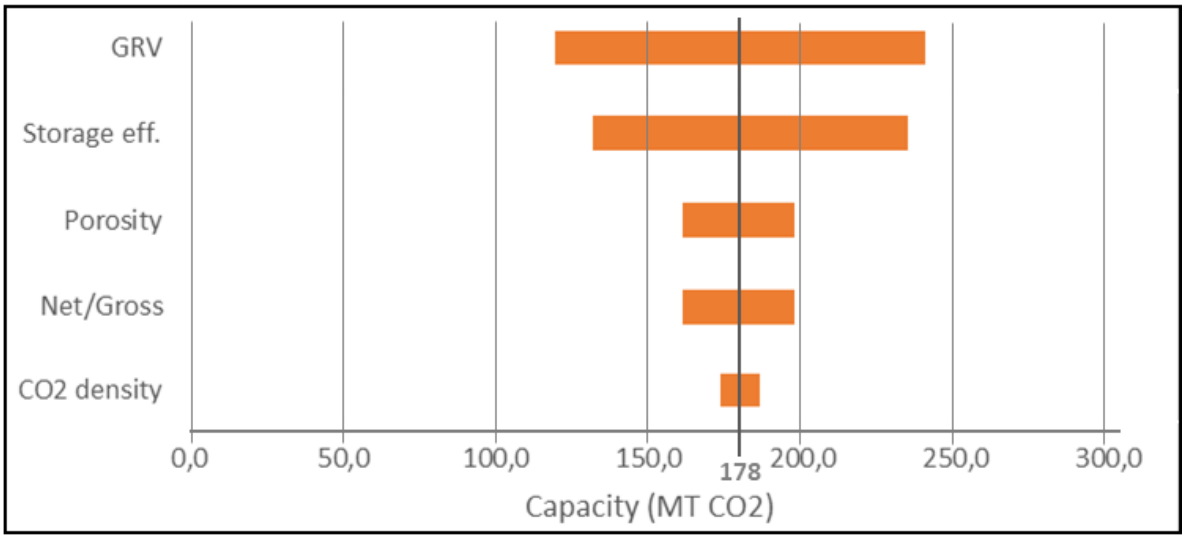

Figure 8.2.2. *Sensitivity (Tornado) plot of how the various input parameters affect the total storage capacity estimate mean (178 MTCO$_2$) of the Gassum reservoir unit. The horizontal bars for each parameter indicate change in storage capacity given that only that parameter is changed leaving all other constant (end levels being P90 and P10, respectively, in the parameter input range).*

8.3 Potential risks

The present report is not a study of geological risks let alone a risk assessment of the Inez structure as potential CO_2storage site. The report is based on updated mapping of important surfaces and geological analyses. Main structural and stratigraphic elements including reservoir-seal pairs, extent/thickness/closure/volume of the storage complex, and larger faults are identified. Some of these identified elements and geological parameters may negatively affect the CO_2 storage potential. This study therefore helps to identify some of the potential geological risk issues. It is recommended to investigate these elements further in future evaluations of the Inez structure, e.g. in specific risk assessment studies.

A frontier prospect like the Inez structure is associated with several such risks. Not all risks can be identified at this early stage, while other risks identified at this early stage will probably turn out to be insignificant once new data have been collected and further investigations have been conducted, which together shed new light on the geology. The three risks listed below is not considered a complete list but rather emphasizes important points that needs further attention in future studies and data collections.

Faulting of the Gassum/Fjerritslev Fm reservoir/seal pair is considered the primary risk at the current level of understanding. First of all, the faults into the Fjerritslev Fm seal introduces a potential risk of vertical leakage from the Gassum Fm that needs to be investigated further when maturing the Inez structure. This also includes investigating the migration pathway of CO_2 leaked from the Gassum reservoir. In the event that CO_2 leaks through the Fjerritslev Fm seal, a possible scenario could be that escaped CO_2 would accumulate in the overlying Haldager Sand Fm that is sealed by the Børglum Fm forming a small four-way closure. If the Inez structure becomes filled to spill point at Haldager Sand level, excess CO_2 may migrate up-dip within the Haldager Sand Fm aquifer towards the east and/or northeast where large positive structures have formed above salt diapirs and salt pillows. How much of the CO_2 that will reach the structures or be left on grain surfaces and trapped in subtle fault traps or retained dynamically in the migration pathway is unknown.

Faulting of the reservoir may be associated with reservoir compartmentalization. About half of the area under closure for the Gassum Fm is densely faulted (Fig. 6.2.2B) with faults situated few hundred meters to few km apart. This may very well reduce reservoir communication and storage efficiency, and thus lower the storage efficiency in these parts and possibly increase the number of required injection wells.

The uncertainty concerning the reservoir quality of the Lower and Middle Triassic Skagerrak Fm at Inez constitutes a third risk. While the Skagerrak Fm is typically sand-prone, thickly developed and of regional extent, reservoir quality varies greatly depending on primary lithologic maturity and diagenesis (Weibel et al. 2017). Diagenesis occurred both near surface shortly after deposition, controlled by an arid to semi-arid climate, and at deep burial and higher temperature and is highly complex in nature. In addition, the migration of fines within the Skagerrak Fm occurred during a well test of the Thisted-2 which also needs to be considered.

9. Conclusions

The Inez structure formed in response to Zechstein salt motion and associated differential subsidence. The salt movements initiated during the Middle Triassic in response to instability introduced by deep-seated extensional faulting. The extension and salt movement increased during the Late Triassic, but Zechstein salt formed a decollement that decoupled deep-seated from shallow-seated faulting. The Inez structure is located between five salt diapirs and a salt pillow. It forms a turtleback structure generated through Mesozoic time in response to migrating rim-synclines formed along the adjacent salt structures.

The Inez structure is cored by a km-thick Permian through Neogene succession. The succession includes three important reservoir-seal pairs: (1) the Skagerrak/Oddesund fms; (2) the Gassum/Fjerritslev fms and (3) the Haldager Sand/Børglum fms. The uppermost Triassic to lowermost Jurassic Gassum Fm forms the primary reservoir in the Inez structure. The formation was deposited in a near-shore environment and is composed by sandstones interbeded with mudstones. The unit was drilled in the Inez-1 well where it forms a 148 m thick unit with a N/G of 0.59 and an average porosity of 20.3% and an average permeability of 442 mD derived from interpretation of electrical logs. The mapped top of the Gassum Fm outlines a roughly 300 km^2 large and 283 m high four-way closure in the Inez area with an apex situated at around 1600 m depth. Small, densely spaced faults offset the Gassum Fm with few tens of meters over part of the structure. The faults typically die out within the overlying Fjerritslev Fm. The Lower Jurassic Fjerritslev Fm mainly consists of claystones and is around 127 m thick in the Inez-1 well. The succession is interpreted to have good sealing capacity although the effect of the small-scale faulting requires further investigation. Assuming an efficient seal, Monte Carlo simulation of the CO_2 storage potential within the Gassum Fm under closure suggest a storage capacity between 104 MT CO_2 (P90) and 264 MT CO_2 (P10) with a mean of around 178 MT CO_2.

The Lower to lowermost Upper Triassic Skagerrak Fm is interpreted seismically in the Inez structure but was not reached by the Inez-1 well. The formation consists of braid plain deposits with a high sandstone content. Based on seismic interpretation, the Skagerrak Fm is interpreted to be thickly developed in the Inez area. The top of the succession delineates a four-way closure around 150 km2 and 175 m high with an apex located in 2500 m depth. By analogy to other Danish wells, and assuming a 300 m Neogene uplift, the succession may hold a good reservoir potential. A storage capacity between 27 MT CO_2 (P90) and 61 MT CO_2 (P10) with a mean of around 43 MT CO_2 has been modelled for the Skagerrak Fm within the Inez structure.

A 9 m thick Jurassic sand-rich interval attributed to the Haldager Sand Fm with an N/G of 0.32, an average sandstone porosity of 0.26 and an average permeability of 871 was intersected from 1522m. The sandstone delineates a roughly 60 km^2 large four-way closure around 39 m high. The sand-prone interval is attributed to the Haldager Sand Fm. A storage capacity between 1.2 MT CO_2 (P90) and 5.5 MT CO_2 (P10) with a mean of around 3.1 MT CO_2 has been modelled for the Haldager Sand Fm. A cumulative storage potential between 149 MT CO_2 (P90) and 310 MT CO_2 (P10) with a mean of around 225 MT CO_2 has been modelled for the entire Inez structure.

The main geological risks identified at this level of maturation and currently available data is associated with the faulting of the Gassum Reservoir and the overlying seal, which first of all introduces a risk for reservoir compartmentalization lowering the efficiency at which CO_2 can be injected into the structure. Secondly, the faulting of at least the lower part of the Fjerritslev Fm

seal may introduce a risk of mechanical weakening and ultimately seal leakage, which requires further investigation.

10. Recommendations for further work

Acquisition of high-quality 3-D seismic data over the Inez structure is an important step towards mitigating the fault-related risks and develop scenarios for an eventual well layout. Such data will also enable a more precise definition of trap closures, reservoir- and seal characterization, depositional facies, faults and depth conversion, which again will feed into a refined storage volume calculation. It is recommended, that a further maturation of the structure should include a risk assessment with seal integrity, and in particular leakage risk at faults and wells should be investigated.

The modelled storage capacity is associated with considerable variability-ranges and uncertainty. In order to mitigate the storage capacity uncertainty and narrow the variability range, first of all, the reservoir gross rock volume of the Inez structure needs to be constrained more accurately e.g. via the collection of 3-D seismic data that could help improve the structural definition, better constrain trap spill points and interpret tops and bases of reservoirs via an improved seismic quality and density, better seismic well ties and a seismic velocity model. In addition, more accurate reservoir parameter could derive from geophysical modelling of 3-D seismic data over the Inez structure and should be complemented by further statistical modelling based on petrophysics and core and cutting analyses. A further key element to quantifying the storage potential of the Inez structure is understanding the storage efficiency. In this study, we have applied an efficiency range from 5% over 10% to 15% introducing a very large storage capacity uncertainty. The storage efficiency factor is mostly dependent on reservoir performance and thus potential heterogeneity, permeability and compartmentalization but also by economic aspects such as well density, well layout and injection design. Better understanding of the reservoir and simulation of reservoir flow could constrain storage efficiency better and thus narrow the estimated final capacity range. Thus, analyses of the physical properties of reservoir and seal are recommended, but also studies of mineralogical, pressure, stress, fault and other effects related to CO_2 injection. While the static storage volume modelled in this study solely addresses the theoretical total storage capacity, it does not address possible storage rates and injection scenarios. This dynamic storage potential is just as important as the static and should be investigated through detailed reservoir modelling with the advent of a more detailed geological understanding of the Inez storage complexes.

A stratigraphic revision of the Skagerrak area is also recommended. The revision of the Gassum Fm thickness from 71 m to 148 m proposed here in the Inez area underlines the importance and potential implications for a regional revision. Such work needs to be carefully worked through integrating petrophysics, paleontology and sedimentology but can be made on existing petrophysical data and cuttings. The revision should address the entire Triassic stratigraphy.

11. References

Bertelsen, F. 1980. Lithostratigraphy and depositional history of the Danish Triassic. Danmarks Geologiske Undersøgelse, DGU Serie B, 4, 59 pp. https://geusjournals.org/index.php/serieb/issue/view/928

Bruno, M.S., Lao, K., Diessl, J. Childers, B., Xiang, J., White, N. & van der Veer, E. 2014. Development of improved caprock integrity analysis and risk assessment techniques. Energy Procedia, 63, 4708 – 4744, doi: 10.1016/j.egypro.2014.11.503.

Chevron. 1978. Completion report: Inez-1 offshore Denmark to Dansk Undergrunds Consortium, Copenhagen, Denmark. 77pp + Encl. 1–3.

Christensen, J.E. & Korstgård, J.A. 1994. The Fjertitslev Fault offshore Denmark-salt and fault interactions. First Break, 12, 31-42.

Clark, C.E. 1962. The PERT model for the distribution of an activity Time. Operations Research 10, pp. 405-406. https://doi.org/10.1287/opre.10.3.405

Frykman, P., Nielsen, L.H., Vangkilde-Petersen, T. & Anthonsen, K. 2009: The potential for large-scale, subsurface geological CO2 storage in Denmark.In: Bennike, O., Garde, A.A. & Watt, W.S. (eds): Review of Survey activities 2008. Geological Survey of Denmark and Greenland Bulletin 17, 13-16.

Fyhn, M.B.W., Gregersen, U., Hjelm, L., Jensen, T.D., Laghari, S., Lauridsen, B.W., Mathiesen, A., Mørk, F., Petersen, H.I. & Rasmussen, L.M. 2022. CCS2022-2024 WP1: The Lisa structure. Seismic data and interpretation to mature potential geological storage of CO2. GEUS Rapport 2022/30.

Hamberg, L., Jepsen, A.-M., Borch, N. Ter, Dam, G., Engkilde, M. K., & Svendsen, J. B. 2007. Mounded structures of injected sandstones in deep-marine Paleocene reservoirs, Cecilie field, Denmark, in A. Hurst and J. Cartwright, eds., Sand injectites: Implications for hydrocarbon exploration and production: AAPG Memoir 87, p. 69 – 79.

Hjelm, L., Anthonsen K., L., Dideriksen, K., Nielsen, C.M., Nielsen, L.H. & Mathiesen A. 2020. Capture, Storage and Use of CO2 (CCUS). Danmarks og Grønlands Geologiske Undersøgelse Rapport 2020/46, 141 pp. https://doi.org/10.22008/gpub/34543

James, B., Grundy, A.T. & Sykes, M.A. 2013. The Depth-Area-Thickness (DAT) Method for Calculating Gross Rock Volume: A Better Way to Model Hydrocarbon Contact Uncertainty, AAPG International Conference & Exhibition. AAPG Search and Discovery Article #90166©2013, Cartagena, Colombia, 8-11 September.

Japsen, P. 1998. Regional velocity-depth anomalies, North Sea chalk: A record of overpressure and Neogene uplift and erosion. AAPG Bulletin 82, 2031–2074. *https://doi.org/10.1306/00aa7bda-1730-11d7-8645000102c1865d*

Japsen, P. Green, P.F., Nielsen, L.H., Rasmussen, E.S. & Bidstrup, T. 2007. Mesozoic–Cenozoic exhumation events in the eastern North Sea Basin: amulti-disciplinary study based on palaeothermal, palaeoburial, stratigraphic and seismic data. Basin Research, 19, 451–490, doi: 10.1111/j.1365-2117.2007.00329.x

Katsube, T.J. & Williamson, M. A. 1994. Effects of diagenesis on shale nano-pore structure and implications for sealing capacity. *Clay Minerals*, 29, 451-461

King, C., Allen, C.O. & Meyrick, R.W. 1978. Inez-1: Final stratigraphical/paleontological report. 32 pp + Encl. 1 & 2.

Mathiesen, A., Dam, G., Fyhn, M.B.W., Kristensen, L., Mørk, F., Petersen, H.I. & Schovsbo, N.H. 2022. Foreløbig evaluering af CO_2 lagringspotentiale af de saline akviferer i Nordsøen. Grønlands Geologiske Undersøgelse Rapport. 2022/15, 151 pp. + App.

McKie, T. 2014. Climatic and tectonic controls on Triassic dryland terminal fluvial system architecture, central North Sea. *In:* A. W. Martinius, R. Ravnås, J. A. Howell, R. J. Steel, and J. P. Wonham (Eds), *Depositional Systems to Sedimentary Successions on the Norwegian Continental Margin*. *Int. Assoc. Sedimentol. Spec. Publ.,* 46, 19–58.

McKie, T. & Williams, B. 2009. Triassic palaeogeography and fluvial dispersal across the northwest European Basins. Geological Journal, 44, 711–741, DOI: 10.1002/gj.1201

Michelsen, O. & Nielsen, L.H., 1991. Well records on the Phanerozoic stratigraphy in the Fennoscandian Border Zone, Denmark. Hans-1, Sæby-1, Terne-1 wells. Danm. geol. Unders., Ser. A, 29, 39 pp.

Michelsen, O. & Nielsen, L.H. 1993. Structural development of the Fennoscandian Border Zone, offshore Denmark. Marine and Petroleum Geology, 10, 124-134.Michelsen, O., Nielsen, L.H., Johannessen, P.H., Andsbjerg, J. & Surlyk, F. 2003. Jurassic lithostratigraphy and stratigraphic development onshore and offshore Denmark. In: Ineson, J.R. and Surlyk, F. (Eds.), The Jurassic of Denmark and Greenland. Geological Survey of Denmark and Greenland Bulletin 1, 145–216. https://doi.org/10.34194/geusb.v1.4651.

Mogensen, T.E. & Jensen, L.N. 1994. Cretaceous subsidence and inversion along the Tornquist Zone from Kattegat to the Egernsund Basin. First Break, 12, 211–222.

Mogensen, TE. & Korstgård, J.A. 2003. Triassic and Jurassic transtension along part of the Sorgenfrei-Tornquist Zone in the Danish Kattegat. In: Surlyk, F., Ineson, J.R. (Eds) he Jurassic of Denmark and Greenland, Geol. Surv. Den. Green. Bull., 1, Copenhagen, 439–458.

Nielsen, L.H. & Japsen, P. 1991. Deep wells in Denmark 1935-1990. Lithostratigraphic subdivision. Danmarks Geologiske Undersøgelse, DGU Serie A, 31, 177 pp.

Nielsen, L.H. 2003. Late Triassic–Jurassic development of the Danish Basin and the Fennoscandian Border Zone, southern Scandinavia. In: Surlyk, F., Ineson, J.R. (Eds) he Jurassic of Denmark and Greenland, Geol. Surv. Den. Green. Bull., 1, Copenhagen, 459–526.

Olivarius, M. & Nielsen, L. H. 2016. Triassic paleogeography of the greater eastern Norwegian–Danish Basin: Constraints from provenance analysis of the Skagerrak Formation. Marine and Petroleum Geology 69, 168-182.

Olivarius, M., Sundal, A., Weibel, R., Gregersen, U., Baig, I., Thomsen, T.B., Kristensen, L., Hellevang, H. & Nielsen, L.H. 2019. Provenance and Sediment Maturity as Controls on CO2 Mineral Sequestration Potential of the Gassum Formation in the Skagerrak. Frontiers in Earth Science, 7. doi:10.3389/feart.2019.00312

Olivarius, M., Vosgerau, H., Nielsen, L.H., Weibel, R., Malkki, S.N., Heredia, B.D. & Thomsen, T.B. 2022. Maturity Matters in Provenance Analysis: Mineralogical Differences Explained by Sediment Transport from Fennoscandian and Variscan Sources. Geosciences, 12, 308. https://doi.org/10.3390/geosciences12080308

Olsen, H. 1988. Sandy braidplan deposits from the Triassic Skagerrak Formation in the Thisted-2 well, Denmark. Danmarks Geologiske Undersøgelse, DGU serie B, 11, 26 pp.

Petersen, H.I., Nielsen, L.H., Bojesen-Koefoed, J.A., Mathiesen, A., Kristensen, L. & Dalhoff, F. 2008. Evaluation of the quality, thermal maturity and distribution of potential source rocks in the Danish part of the Norwegian–Danish Basin. Geol. Surv. Denm. Greenl. Bull. 16, 66.

Petersen, H.I & Smit, F.W.H. 2023. Application of mud gas data and leakage phenomena to evaluate seal integrity of potential CO_2 storage sites: a study of chalk structures in the Danish Central Graben, North Sea. Journ. Petrol. Geol. 46, 47–76.

Petersen, H.I., Springer, N., Weibel, R. & Schovsbo, N.H. 2022. Sealing capability of the Eocene–Miocene Horda and Lark formations of the Nini West depleted oil field – implications for safe CO_2 storage in the North Sea. Int. Journ. Greenh. Gas Contr. 118, doi.org/10.1016/j.ijggc.2022.103675

Phillips, T.B., Jackson, C.A-L., Bell, R.E. & Duffy, O.B. 2018. Oblique reactivation of lithosphere-scale lineaments controls rift physiography – the upper-crustal expression of the Sorgenfrei–Tornquist Zone, offshore southern Norway. Solid Earth, 9, 403–429, https://doi.org/10.5194/se-9-403-2018

Span, R. & Wagner, W. 1996. A new equation of state for carbon dioxide covering the fluid region from the triple-point temperature to 1100K at pressures up to 800 MPa, J. Phys. Chem. Ref. Data., 25, 1509-1596 PP.

Springer, N., Lotentzen, H., Fries, K. & Lindgreen, H. 2010. Caprock seal capacity evaluation of the Fjerritslev and Børglum Formations. Contribution to the EFP-project AQUA-DK. Danmarks og Grønlands Geologiske Undersøgelse Rapport nr. 112.

Statoil, 1988. Completion report Well 5408/18 – 1.1A Licence 8/86 Felicia. 134 pp & App. I-III.

Stemmerik, L., Ineson, J.R. & Mitchell, J.G., 2000: Stratigraphy of the Rotliegend Group in the Danish part of the Northern Permian Basin, North Sea. Journal of the Geological Society, London, 157, 1127-1136.

Surlyk, F., Dons, T. Clausen, C.K. & Higham, J. 2003. Upper Cretaceous. In: Evans, D., Graham, C., Armour, A., Bathurst, P., (Eds) The millennium Atlas: Petroleum geology of the central and northern North Sea. Geol. Soc., London, 213–233 pp.

Sørensen, M.B., Voss, P.H., Havskov, J., Gregersen, S. and Atakan, K. 2011. The seismotectonics of western Skagerrak. Journal of Seismology, 15, 599-611.

Van Buchem, F.S.P., Smit, F.W.H., Buijs, G.J.A., Trudgill, B. & Larsen, P.-H. 2018. Tectonostratigraphic framework and depositional history of the Cretaceous–Danian succession of the Danish Central Graben (North Sea) – new light on a mature area. Geol. Soc. London, Pet. Geol. Conf. Ser. 8, 9–46.

Vejbæk, O.V., 1997. Dybe strukturer i danske sedimentære bassiner. Geologisk Tidsskrift, 4, pp. 1-31. https://2dgf.dk/xpdf/gt1997-4-1-31.pdf.

Vejbæk, O. & Andersen, C. 2002. Post mid-cretaceous inversion tectonics in the Danish Central Graben - regionally synchronous tectonic events? Bull. Geol. Soc. Denmark 49, 139–144.

Wang, Y., Zhangb, K. & Wua, N. 2013. Numerical Investigation of the Storage Efficiency Factor for CO2 Geological Sequestration in Saline Formations, Energy Procedia, Volume 37, 2013, 5267-5274 PP.

Weibel, R., Olivarius, M., Kjøller, C., Kristensen, L., Hjuler, M.L., Friis, H., Pedersen, P.K., Boyce, A., Andersen, M.S., Kamla, E., Boldreel, L.O., Mathiesen, A. & Nielsen, L.H. 2017. The influence of climate on early and burial diagenesis of Triassic and Jurassic sandstones from the Norwegian–Danish Basin. Depos. Rec., 3, 60–91.

Vosgerau, H., Gregersen, U., Hjuler, M.L., Holmslykke, H.D., Kristensen, L., Lindström, S., Mathiesen, A., Nielsen, C.M., Olivarius, M., Pedersen, G.K. & Nielsen, L.H. 2016. Reservoir prognosis of the Gassum Formation and the Karlebo Member within two areas of interest in northern

Copenhagen. The EUDP project “Geothermal pilot well, phase 1b”. GEUS Rapport 2016/56. 138 pp + app 1–5. https://doi.org/10.22008/gpub/32477